AWARD NUMBER: W81XWH-21-1-0540

TITLE: Targeting De Novo NAD+ Synthesis Through the Kynurenine Pathway in Renal Cell Carcinoma

PRINCIPAL INVESTIGATOR: George Sutphin

CONTRACTING ORGANIZATION: University of Arizona, Tucson, AZ

REPORT DATE: November 2023

TYPE OF REPORT: Final

PREPARED FOR: U.S. Army Medical Research and Development Command
Fort Detrick, Maryland 21702-5012

REPORT DOCUMENTATION PAGE

Form Approved
OMB No. 0704-0188

1. REPORT DATE	2. REPORT TYPE	3. DATES COVERED
November 2023	Final	01Aug2021-31Jul2023

4. TITLE AND SUBTITLE

Targeting De Novo NAD+ Synthesis Through the Kynurenine Pathway in Renal Cell Carcinoma

5a. CONTRACT NUMBER

5b. GRANT NUMBER
W81XWH-21-1-0540

5c. PROGRAM ELEMENT NUMBER
KC200067

6. AUTHOR(S)
Sutphin, George

E-Mail:

5d. PROJECT NUMBER

5e. TASK NUMBER

5f. WORK UNIT NUMBER

7. PERFORMING ORGANIZATION NAME(S) AND ADDRESS(ES)
Arizona Board of Regents, University of Arizona
Sponsored Projects Services
PO Box 210158B, Rm 538
Tucson, AZ 85721-1508

8. PERFORMING ORGANIZATION REPORT NUMBER

9. SPONSORING / MONITORING AGENCY NAME(S) AND ADDRESS(ES)

U.S. Army Medical Research and Development Command
Fort Detrick, Maryland 21702-5012

10. SPONSOR/MONITOR'S ACRONYM(S)

11. SPONSOR/MONITOR'S REPORT NUMBER(S)

12. DISTRIBUTION / AVAILABILITY STATEMENT

Approved for Public Release; Distribution Unlimited

13. SUPPLEMENTARY NOTES

14. ABSTRACT

Cancer cells alter their metabolism to meet the energetic and biosynthetic demands of malignant tumors and evade immune surveillance. Renal cell carcinomas (RCC) undergo substantial metabolic remodeling are considered a metabolic disease by some researchers. The kynurenine pathway converts tryptophan to nicotinamide adenine dinucleotide (NAD+) and is commonly activated in RCC. Kynurenine metabolism shows promise as both a mechanistic driver of pathology and a therapeutic target. Kynurenine metabolism provides two advantages to tumor cells: tryptophan depletion in the local microenvironment suppresses T cells while NAD+ production supports high energy and redox demands. Tryptophan-mediated immune evasion is widely studied while the role of de novo NAD+ synthesis has been relatively neglected. We hypothesized that preventing NAD+ synthesis via kynurenine metabolism would inhibit RCC and progression. We tested this hypothesis by knocking down three kynurenine pathway enzymes—HAAO, KMO, and QPRT—in RCC cell lines and measured malignant phenotypes both in vitro (Aim 1) and in vivo (Aim 2). RCC cell lines lacking HAAO, but not KMO or QPRT, exhibited several metrics of increased proliferation in culture. Surprisingly, RCC cell lines lacking all three enzymes produced tumors that were less lethal in vivo, suggesting that these modifications produce less aggressive tumors.

15. SUBJECT TERMS

Renal cell carcinoma, RCC, kidney cancer, tryptophan, NAD+, kynurenine, metabolism, metabolic remodeling

16. SECURITY CLASSIFICATION OF:			17. LIMITATION OF ABSTRACT	18. NUMBER OF PAGES	19a. NAME OF RESPONSIBLE PERSON
a. REPORT	b. ABSTRACT	c. THIS PAGE			USAMRDC
Unclassified	Unclassified	Unclassified	Unclassified	38	19b. TELEPHONE NUMBER *(include area code)*

TABLE OF CONTENTS

1. INTRODUCTION:

Metabolic reprogramming is a hallmark of cancer and a prominent feature of renal cell carcinoma (RCC). *De novo* synthesis of nicotinamide adenine dinucleotide (NAD^+) through the kynurenine pathway is abnormally activated in RCC and represents a promising therapeutic target. The purpose of this work is to determine the impact of knocking down three enzymes in this pathway (HAAO, KMO, and QPRT) on RCC malignancy.

2. KEYWORDS:

Renal cell carcinoma, RCC, kidney cancer, tryptophan, NAD^+, kynurenine, metabolism, metabolic remodeling

3. ACCOMPLISHMENTS:

What were the major goals of the project?

Specific Aim 1. Characterize the relationship between kynurenine pathway activity, NAD^+ availability and downstream processes, and malignant phenotypes in RCC cell lines.

- **Major Task 1.1. Obtain and validate renal carcinoma cell (RCC) lines with reduced expression of *KYNU*, *ACMSD*, and *QPRT*.** (Completion: 100%, Original Timeline: months 1-5; Completion: Month 12).

- **Major Task 1.2. Characterize novel *KYNU*, *ACMSD*, and *QPRT* knockout Renca^{Luc} cell lines and compare to parallel measurements in unmodified cells.** (Completion: 100%, Original Timeline: months 3-6; Completion: Month 18).

- **Major Task 1.3. Characterize the impact of siRNA knockdown of *KYNU*, *ACMSD*, and *QPRT* on RPTEC (non-malignant control), 786-O, Caki-1, and ACHN cell lines and compare to cells treated with scrambled siRNA (negative control).** (Completion: 100%, Original Timeline: months 6-11; Completion: Month 21).

Specific Aim 2. Evaluate the impact of impaired kynurenine metabolism on preclinical RCC progression.

- **Major Task 2.1. Complete administrative and training requirements for mouse studies.** (Completion: 100%, Original Timeline: months 1-5; Estimated Completion: Month 15).

- **Major Task 2.2. Complete survival study for mice following Renca^{Luc} cell challenge.** (Completion: 100%, Original Timeline: months 6-10; Estimated Completion: Month 22).

- **Major Task 2.3. Complete cross-sectional study for mice following Renca^{Luc} challenge.** (Completion: 100%, Original Timeline: months 7-11; Completion: Month 23).

Reporting.

- **Major Task 3.1.** Submit manuscript and compile data for final report and presentation. (Completion: 100%, Original Timeline: months 4-12; Completion: Month 24).

What was accomplished under these goals?

** Figures are provided at the end of the Accomplishments.

Specific Aim 1. Characterize the relationship between kynurenine pathway activity, NAD^+ availability and downstream processes, and malignant phenotypes in RCC cell lines.

In Year 1 we made minor modifications to the approach in this Aim, specifically expanding the initial set of enzymes to include knockdown of the enzyme HAAO and supplementation with the HAAO substrate, 3HAA, and examination of the impact of each kynurenine pathway intervention on selected cellular phenotypes in the context of ferroptosis induction by sorafenib, sulfasalazine, or erastin (see CHANGES/PROBLEMS for additional detail). Ferroptosis is a form of non-apoptotic cell death driven by iron-dependent lipid peroxidation. Cells combat ferroptosis by limiting lipid peroxidation via increasing production of the antioxidant glutathione (GSH) through activation of the NRF2 transcription factor. These changes were motivated by parallel work in *Caenorhabditis elegans* in the context of aging, immune function, and stress response. Specifically, we find a that inhibition of HAAO or supplementation with 3HAA activates the NRF2/SKN-1-glutathione stress response pathway (**Figure 1**), which is intimately linked with ferroptosis. Induction of ferroptosis is a major area of study as a treatment strategy for RCC, as well other cancer types. We further find that NRF2/SKN-1 activation is partially dependent on the mitochondrial aconitase (**Figure 2**) and that kynurenine interventions can influence mitochondrial dynamics in *C. elegans* (**Figure 3**), providing a directly link to the NAD^+-linked mitochondrial processes that we are examining in this work.

Major Task 1.1. Obtain and validate renal carcinoma cell (RCC) lines with reduced expression of *KYNU*, *ACMSD*, and *QPRT*.

We ordered and validated, or in some cases obtained internally validated, human control (RPTEC) and RCC (786-O, Caki-1, and ACHN) cell lines immediately after the award was funded (*Subtask 1.1.1*). For the human cell lines, we have validated our capacity to knockdown (siRNA or pharmacological inhibition) enzymes or supplement the substrate metabolite (*Subtask 1.1.3*).

For the mouse cells, we similarly obtained and validated Renca^{Luc} cells and submitted them to our core facility to generate the *Kynu*, *Acmsd*, and *Qprt* (*Subtask 1.1.2*). We ended up adding *Haao* and *Kmo* knockout cells to our initial list funded through an independent source, since the CRISPR process was being conducted for two genes in parallel. Technical complications resulted in only the *Haao* knockout being successful on the first pass, and the other taking additional troubleshooting. After a substantial delay relative to the original timeline (nearly 12 months from project start, rather than 4-6 weeks), we know have four knockout cell lines (two *Haao*, one *Kmo*,

and one *Qprt*). While the specific gene set is different, the goal of inhibiting the kynurenine pathway at different points in the process is achieved and this task is complete.

Major Task 1.2. Characterize novel *KYNU*, *ACMSD*, and *QPRT* knockout Renca^{Luc} cell lines and compare to parallel measurements in unmodified cells.

Accomplishments for Major Tasks 1.2 and 1.3 are closely related and reported together in the next section.

Major Task 1.3. Characterize the impact of siRNA knockdown of *KYNU*, *ACMSD*, and *QPRT* on RPTEC (non-malignant control), 786-O, Caki-1, and ACHN cell lines and compare to cells treated with scrambled siRNA (negative control).

As above, this work focuses on cells with knockdown of *Haao*, *Kmo*, and *Qprt*, which were the lines with successful knockout. Based on our promising preliminary data with 3HAA, we also evaluated cells supplemented with 3HAA. These represent minor changes from the original proposal that are in line with the project goals (see Major Task 1.1). LC-MS/MS data reveals a modest decrease in NAD^+ in each cell line with reduced kynurenine pathway activity and the expected pattern of changes in other kynurenine pathway metabolites given the location of each enzyme (i.e., the immediate upstream metabolite increases substantially, downstream metabolites decrease, and some metabolites further upstream increase modestly). We did have technical challenges harvesting sufficient cells for these measurements and some metabolites were below the detection threshold; however, the patterns observed agree with published data and our earlier data in both worms and mouse tissue, which validates the cell lines (*Subtask 1.2.1, 1.3.1*; data not shown). In early experiments examining siRNA knockdown of kynurenine pathway enzymes, we found that (perhaps as expected) the outcomes had a higher degree of variance compared to the CRISPR knockout Renca^{Luc} lines, requiring additional validation. For this reason, we focused on the Renca^{Luc} KO lines for primary inquiry and confirmed key observations with siRNA, which generally agreed (except were otherwise noted).

We characterized several aspects of growth in Renca^{Luc} cells (*Subtasks 1.2.2, 1.3.2*). *Haao* knockout accelerates the ability of Renca^{Luc} cells to recolonize available culture media in a scratch/wound healing assay, while knockout of either *Kmo* or *Qprt* has the opposite effect (**Figure 4**). Cell count was not different between cultured cell lines over time (*Kmo*$^{-/-}$ cells had a trend toward lower cell count that was not significant; **Figure 5**). Transwell assays did not reveal a significant difference between strains in migratory potential, however, *Haao*$^{-/-}$ trended toward increased migration while *Kmo*$^{-/-}$ and *Qprt*$^{-/-}$ cells trended toward decreased migratory potential (**Figure 6**). In colony formation assays, *Kmo*$^{-/-}$ cells trended toward increased colony number, while *Haao*$^{-/-}$ cells (cell line A31) displayed a substantial and increase in colony size (**Figure 7**); however, the second, independently generated *Haao*$^{-/-}$ cell line (cell line A28) did not show increased colony size, suggesting underlying genetic or epigenetic differences between these cell lines (**Figure 7**). Taken together, these assays suggest that knockout of *Haao* may increase aggressive cellular behavior in Renca^{Luc} cells by promoting migratory behavior, and possibly by increasing cellular growth or proliferation depending on environmental factors such as cell density (since *Haao*$^{-/-}$ cells displayed a trend toward increased migration in the transwell assays and filled in the area void of cells in the wound healing assay more rapidly than wild type) or local extracellular matrix (since *Haao* cells displayed increased colony size in the colony formation assay, which is conducted on

soft agar). However, given the variability and lack of significance in several of these measurements, these results will require further validation.

Cells lacking *Haao* accumulate 3HAA. Given the observed changes in cell behavior in response to *Haao* knockdown and our observations linking 3HAA to oxidative stress and NRF2/SKN-1 in *C. elegans*, we further examined the impact of 3HAA on cell growth and proliferation, and the interaction between 3HAA and ferroptosis. As noted above, *Haao* knockout accelerates the ability of Renca^{Luc} cells to recolonize available culture media in a scratch/wound healing assay (**Figure 8**). Interestingly, this effect is repressed by limiting the fetal bovine serum in the media, while 3HAA supplementation modestly inhibits colonization in the low FBS condition (**Figure 8**). Supplementing human RCC with 3HAA modestly increases cell growth for some RCC cell lines but not others, consistent with a model where in reduced *Haao* promotes cell growth via elevated 3HAA (**Figure 9**).

In the context of ferroptosis, we initially found that *Haao* knockout modestly sensitizes Renca^{Luc} cells to sorafenib, a tyrosine kinase inhibitor that is known to induce ferroptosis (through it also impacts unrelated pathways; **Figure 10D**). Around the same time, we similarly found through and independently funded pilot study that 3HAA supplementation sensitized the hepatocellular carcinoma SK-Hep1 cells to sulfasalazine (**Figure 10C**), and in particular induced a ballooning phenotype in dying cells that is characteristic of ferroptotic cell death (**Figure 10B**). Sulfasalazine is known to induce ferroptosis by inhibiting cystine import, a rate-limiting precursor in the GSH production process. 3HAA also induced expression of NRF2in these cells (**Figure 10A**), in agreement with our observations in *C. elegans* (**Figure 1**) and supporting a role for the NRF2-gluthione oxidative stress response in modulating cellular growth phenotypes in response to HAAO or 3HAA manipulation. To further dissect the role of 3HAA in ferroptosis, we examined the impact of supplementing cells with 3HAA followed by challenge with hydrogen peroxide or paraquat to directly promote oxidative stress and lipid peroxidation. Interestingly, the impact of 3HAA in this context was inconsistent. In some cell lines 3HAA had no effect on sensitivity to oxidative stress, while in others it increased sensitivity (**Figure 11**). We next examined the impact of 3HAA on ferroptosis induced by either erastin or RSL3. Similar to Sorafenib, erastin induces ferroptosis by inhibiting cystine import, but is more specific and does not have other know off-target effects. RSL3 promotes lipid peroxidation by directly inhibits GPX4, which prevents cells from utilizing GSH as an antioxidant. In contrast to Sorafenib and sulfasalazine, 3HAA induced resistance of RCC cell lines to erastin and RSL43 (**Figure 12**). Erastin sensitivity is, in part, dependent on whether cells are exposed to 3HAA prior to vs. concurrent with erastin, suggesting 3HAA may induce an adaptation that impacts ferroptosis sensitivity (**Figure 13**). This latter finding is in agreement with two recent publications from other laboratories that report 3HAA-induced ferroptosis resistance (PMID: 36627132, PMID: 35245456). These studies suggest that 3HAA is promoting ferroptosis resistance by generating reactive oxygen species and thereby activating NRF2. The canonical route for activation of the NRF2-GSH pathway is through oxidation of the NRF2-bound KEAP1 subunit of the E3 ubiquitin ligase, releasing NRF2 to translocate to the nucleus and initiate transcription of target genes, including the genes that produce and utilize GSH (**Figure 14B**). While not strictly part of this work, in a parallel study using immortalized human embryonic kidney cells (Hek293T/17), hepatocellular carcinoma (SK-Hep1), and pancreatic cancer (PANC-1) cells, we find that 3HAA supplementation or HAAO inhibition with the 3HAA analog 4Cl-3HAA activate NR2 (**Figure 14A**), but actually reduces endogenous reactive oxygens species (**Figure 14C-E)**, suggesting that NRF2 activation is mediated by a mechanism independent of reactive oxygen species. Supporting this idea, in *C. elegans* we find both oxidative stress dependent and independent activation of

NRF2/SKN-1 by 3HAA (data not shown). Taken together, these data point to a more complicated interaction between 3HAA and ferroptosis that may depend on the initial levels or ROS, GSH, and NRF2 activation in the cells. Ferroptosis is also dependent on the availability of labile iron. We and others have linked 3HAA to cellular iron homeostasis. In ongoing work we are exploring the mechanisms linking 3HAA to iron regulation and we anticipate that the findings will have important implications that my help clarify the impact of 3HAA on ferroptosis.

Finally, around the time that this project was awarded, we were conducting independently funded pilot studies with human liver (SK-Hep1), kidney (Hek293T/17), and pancreas (Panc-1) cell lines looking at aspects of interaction between kynurenine pathway interventions and mitochondrial function. We utilized the Hek293T/17 cells to begin optimizing protocols while we were working to obtain the RCC cell lines for this work. We found that supplementing media with either exogenous 3HAA or the HAAO inhibitor 4Cl-3HAA resulted in a reduction in mitochondrial membrane potential after 48 hours (**Figure 15**), which is consistent with a modest decrease in NAD^+. Preliminary data from Western blots suggest that both interventions can activate the mitochondrial fission protein DRP-1 (data not shown), in agreement with our observations of increased mitochondrial fission in *C. elegans* (**Figure 3**) and human RCC cells (**Figure 16**). We did not observe changes in mitochondrial respiration (*Subtask 1.2.3, 1.3.3*).

Specific Aim 2. Evaluate the impact of impaired kynurenine metabolism on preclinical RCC progression.

Major Task 2.1. Complete administrative and training requirements for mouse studies.

This task was preparatory for Major Tasks 2.2 and 2.3. Our internal IACUC amendment for this work was approved midway through Year 1. When we sent the approved document for ACURO approval we were too close to our internal 4-year review and *de novo* renewal for the overall protocol and ACURO would not accept the submission and was delayed. Following our IACUC *de novo* renewal we successfully submitted the protocol to ACURO and it was approved early in Year 2 (*Subtask 2.1.1*). All staff who conducted mouse work completed general surgical training and hand-on training for the specific surgical procedure through our Experimental Mouse Shared Resource (EMSR), who have extensive experience with mouse kidney surgery (*Subtask 2.1.2*).

Major Task 2.2. Complete survival study for mice following Renca^{Luc} cell challenge.

Accomplishments for Major Tasks 2.2 and 2.3 are closely related and reported together in the next section.

Major Task 2.3. Complete cross-sectional study for mice following Renca^{Luc} challenge.

During Year 2 we acquired BALB/cByJ mice from The Jackson Laboratory (*Subtasks 2.2.1, 2.3.1*) and conducted studies to both assess survival and kidney tissue metrics following injection of Renca^{Luc} *Haao*, *Kmo*, and *Qprt* knockout cell lines orthotopically. Renca cells were originally isolated from an RCC tumor from a Balb/c mouse. This approach is there for syngeneic and allows tumor progression to be monitored in the presence of an active immune system without tumor cells being rejected as foreign. Based on the cellular data (Major Tasks 1.2, 1.3), we anticipated *Haao*$^{-/-}$

Renca^{Luc} cells to produce more aggressive tumors, reducing animal survival and increasing tumor growth. Surprisingly, mice receiving each of the knockout Renca^{Luc} cell lines had improved survival relative to mice receiving unmodified Renca^{Luc} cells (**Figure 17**). Tumor genotype did not impact body weight (**Figure 18**). Consistent with the survival data, *Haao*$^{-/-}$ tumors were smaller throughout the study (**Figure 19B**), as measured by bioluminescence (**Figure 19A**), and all three-tumor genotype resulted in fewer detectable metastatic events, with *Haao*$^{-/-}$ tumors producing the fewest metastases (**Figure 19C**). *Kmo*$^{-/-}$ cells showed a trend toward producing larger tumors that only reached significance during the second week (**Figure 19B**). Tumor kynurenine metabolite levels showed similar trends to the *C. elegans* and cultured cells (not shown) and collected tissue weights were similar across tumor genotypes (**Figure 20**; liver and lung were examined as common metastasis sites for Renca cells). Unfortunately, a processing error resulted in loss of samples collected for histology. Taken together, our *in vivo* data tended to suggest that RCC tumors deficient in kynurenine metabolism tend to be less aggressive than tumors with normal kynurenine metabolism. This is the opposite outcome that we predicted from our cell culture data, which suggests that standard cell culture does not capture some aspects of the tumor microenvironment that are relevant to tumor behavior. Based on what is known about kynurenine metabolism and the specific pattern of phenotypes in our cellular data, clear candidates include the presence of immune cells, the presence of normal cells with intact kynurenine metabolism, and the specific characteristics of each tumor with respect to NAD^+ levels, iron metabolism, NRF2 pathway activation, GSH levels, and reactive oxygen species. We compared our mouse data to publicly available human RCC data, and found that gene expression of *KMO*, *HAAO*, and *QPRT* in RCC tumors does not consistently predict patient survival (**Figure 21**), further supporting the idea that tumor type and the specific kynurenine pathway mutation may be important considerations. We intend to explore several of these avenues in ongoing and future work.

Reporting.

Major Task 3.1. Submit manuscript and compile data for final report and presentation.

This work supports three publications. The cellular phenotypes reported here made a minor contribution to a manuscript describing the relationship between 3HAA, reactive oxygen species production, and activation of the NRF2 oxidative response pathway, and is available on bioRxiv pending submission to Redox Biology in early 2024 (DOI:10.1101/2023.02.16.528568). The second manuscript describes the interaction between 3HAA and ferroptosis in a range of cancer cells, and is in final preparation for submission in early 2024. The third describes the impact of knocking out kynurenine pathway enzymes on the behavior and *in vivo* tumor progression of Renca^{Luc} cells, which was entirely supported by this award, and is in preparation for submission by mid-2024.

What opportunities for training and professional development has the project provided?

Jose Raul Castro-Portuguez (PhD Students) attended the American Aging Association (AGE) Annual Meeting in San Antonio in 2022, the Gerontological Society of America (GSA) Annual Meeting in Indianapolis in 2022, and in Oklahoma City in 2023. He has become active in the trainee chapters in both societies and developed many professional relationships, in large part stemming from interest in his work on kynurenine metabolism and its interaction with the NRF2-

glutathione-ferroptosis axis. He has also presented aspects of this work as part of several oral presentations at retreats and seminars on the University of Arizona campus.

How were the results disseminated to communities of interest?

Presentation at the AGE and GSA annual meetings. Manuscripts are in preparation for publication.

What do you plan to do during the next reporting period to accomplish the goals?

Nothing to report.

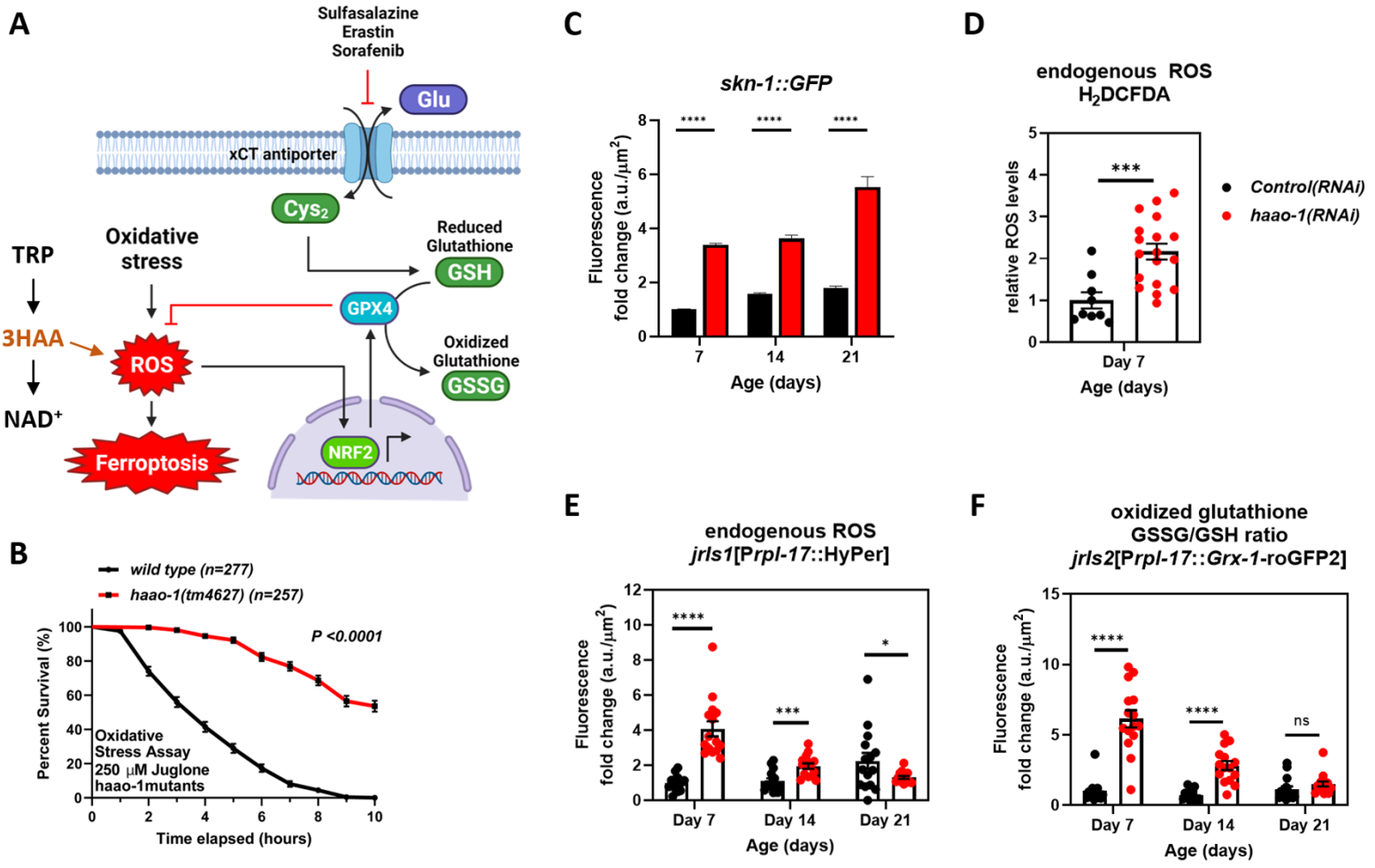

Figure 1. Knockdown of *haao-1* promotes oxidative stress resistance by hormetic activation of the Nrf2/SKN-1-glutathione oxidative stress response pathway in *Caenorhabditis elegans*. (**A**) Model linking HAAO/HAAO-1 inhibition to Nrf2/SKN-1 activation via mild upregulation of reactive oxygen species (ROS) through increased 3-hydroxyanthranilic acid (3HAA) concentrations. (**B**) Worms lacking functional *haao-1* are resistant to acute juglone toxicity. RNAi knockdown of *haao-1* increases expression of Nrf2/SKN-1 (**C**), elevates endogenous ROS (**D**, **E**), and elevates the oxidized glutathione ratio (GSSG/GSH; **F**).

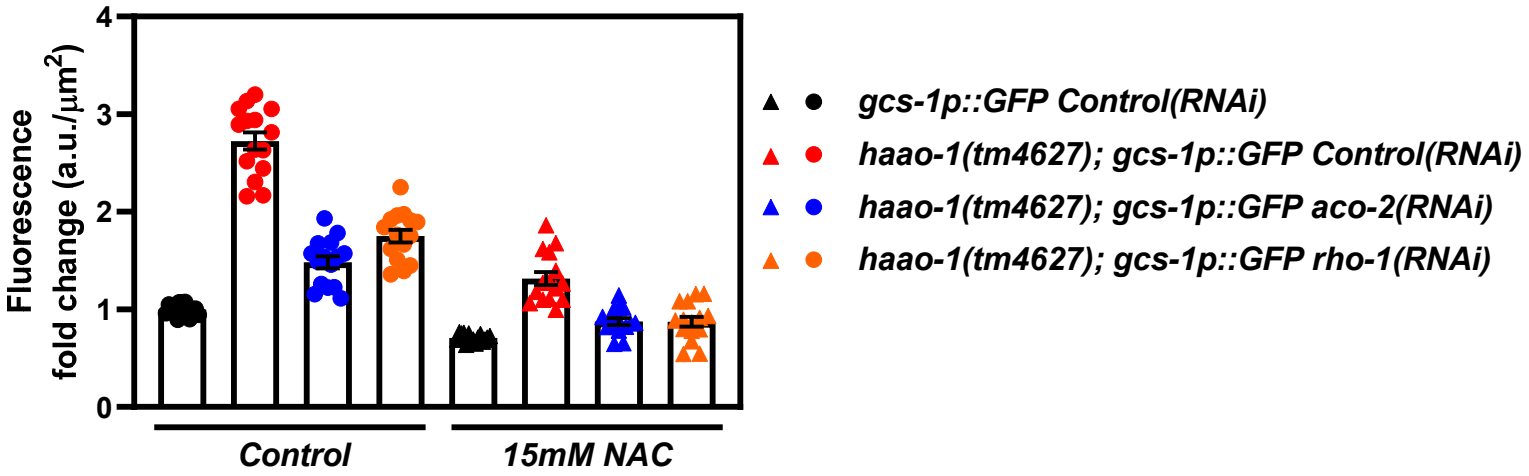

Figure 2. Suppression of ROS with N-acetyl cysteine (NAC) in combination with knockdown of mitochondrial aconitase (ACO-2) or the rho GTPase (RHO-1) is sufficient to suppress activation of Nrf2/SKN-1 by *haao-1* in *C. elegans.* Expression of the Nrf2/SKN-1 target gene GCS-1, as measured by a GFP expressed on the *gcs-1* promotor, is activated by deletion of *haao-1*. This activation is suppressed by 15 mM exogenous NAC in the worm media in combination with RNAi knockdown of either *aco-2* or *rho-1*.

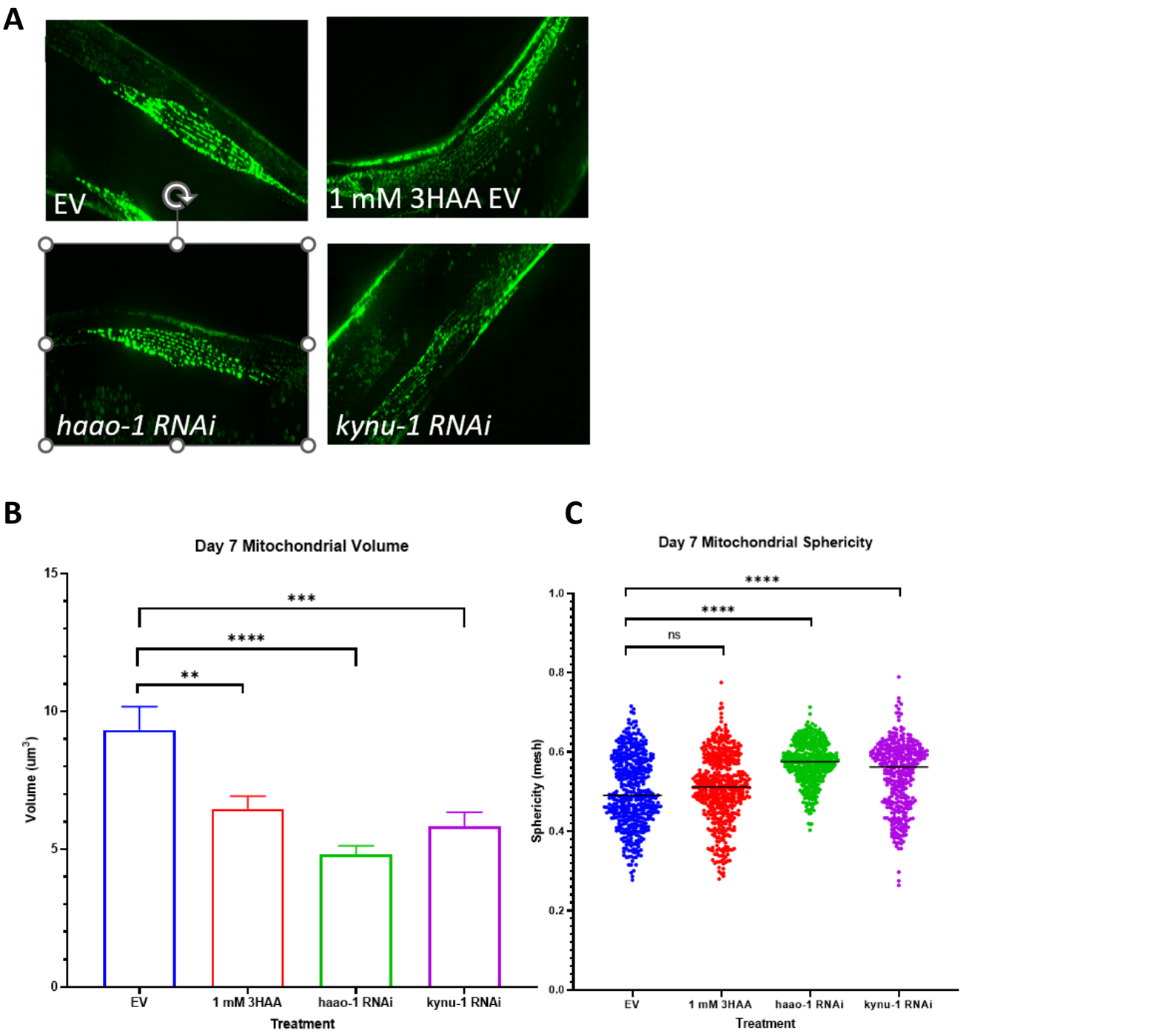

Figure 3. Kynurenine pathway modulation promotes mitochondrial fission in *C. elegans.*
(**A**) Representative images of *C. elegans* transgenically expressing mitochondria-targeted GFP in body wall muscle (*myo-3p::GFP(mito)*) in response to empty vectore (EV) RNAi, supplementation with 1 mM 3HAA, *haao-1(RNAi)*, or *kynu-1(RNAi)*. (**B**) RNAi knockdown of *haao-1* or *kynu-1,* or supplementation with 1 mM 3HAA, decreases overall mitochondria volume. (**C**) RNAi knockdown of *haao-1* or *kynu-1*, but not supplementation with 1 mM 3HAA, increases sphericity of individual mitochondrial fragments, a metric of increased mitochondrial fission.

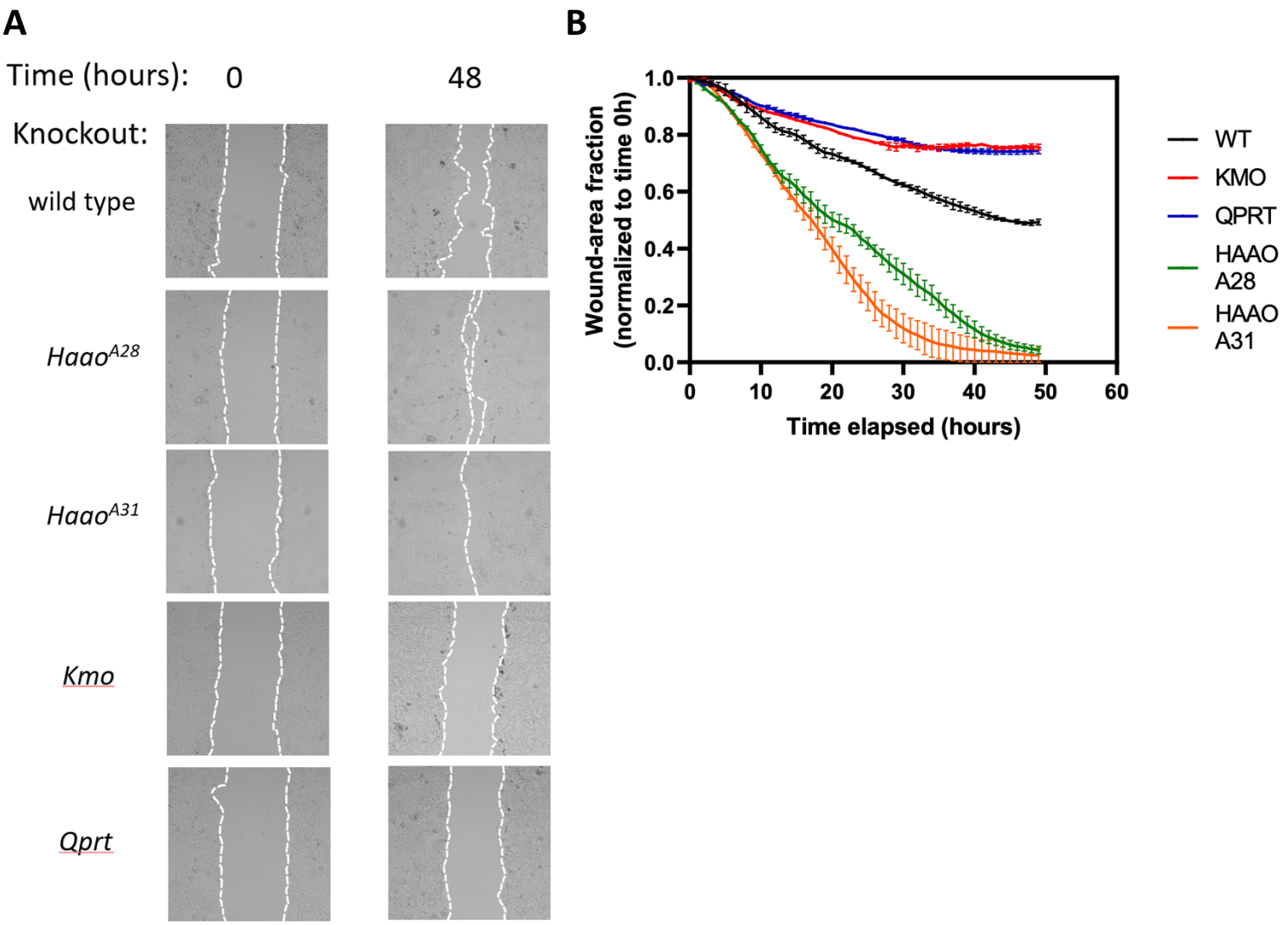

Figure 4. Knocking out different kynurenine pathway enzymes differentially impacts migration and/or proliferation of Renca^{Luc} cells. *Haao*$^{-/-}$ Renca^{Luc} cells more rapidly colonize available culture area than wild type cells in a scratch/wound healing assay when cultured in 10% FBS. In contrast, *Kmo*$^{-/-}$ and *Qprt*$^{-/-}$ Renca^{Luc} cells more slowly colonize available culture area than wild type cells in a scratch/wound healing assay when cultured in 10% FBS. (**A**) representative images of scratch assays at 0 and 48 hours. (**B**) Automated quantification of would area for images taken at 20-minute intervals for 72 hours following initiation of the scratch. All values are normalized to the initial scratch area.

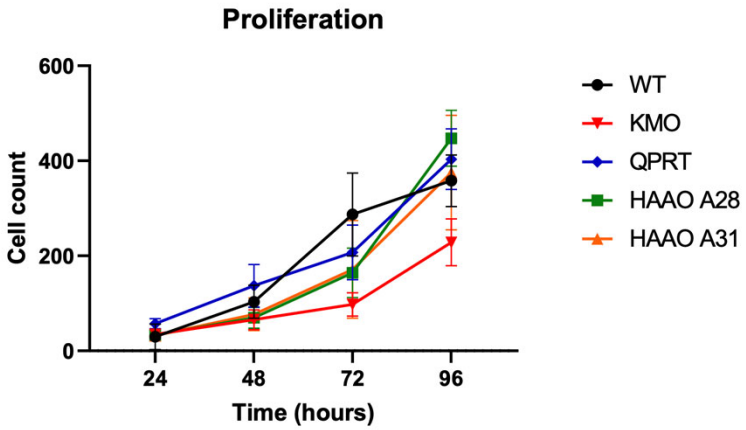

Figure 5. Renca^{Luc} cell proliferation in culture is not affected by knockout of *Haao*, *Kmo*, or *Qprt*. Cell proliferation, as measured by cell counts over time for Renca^{Luc} cells cultured in 10% FBS, is not significantly affected by knockout of *Haao, Kmo*, or *Qprt*$^{-/-}$ Renca^{Luc}.

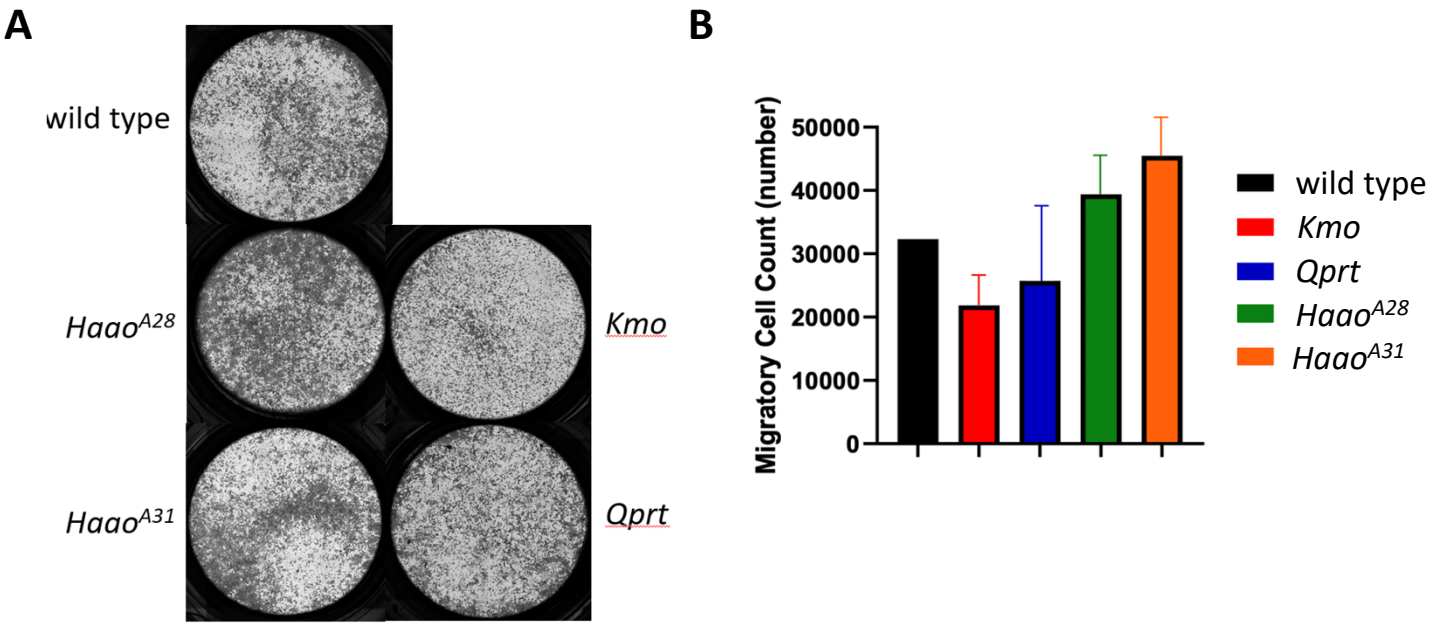

Figure 6. Cells lines with knockout of *Haao*, *Kmo*, or *Qprt* show trends toward differential migration potential. *Haao*$^{-/-}$ Renca^{Luc} cells show a trend toward increased migration potential, while *Kmo*$^{-/-}$ cells show a trend toward decreased migration, but neither reached significance. Migration is estimated by measuring the number of cells that pass through a porous membrane in response to a chemoattractant (10% FBS; cell density in the images shown). (**A**) Representative images of migrated cells. (**B**) Quantification of migratory cell number in each image.

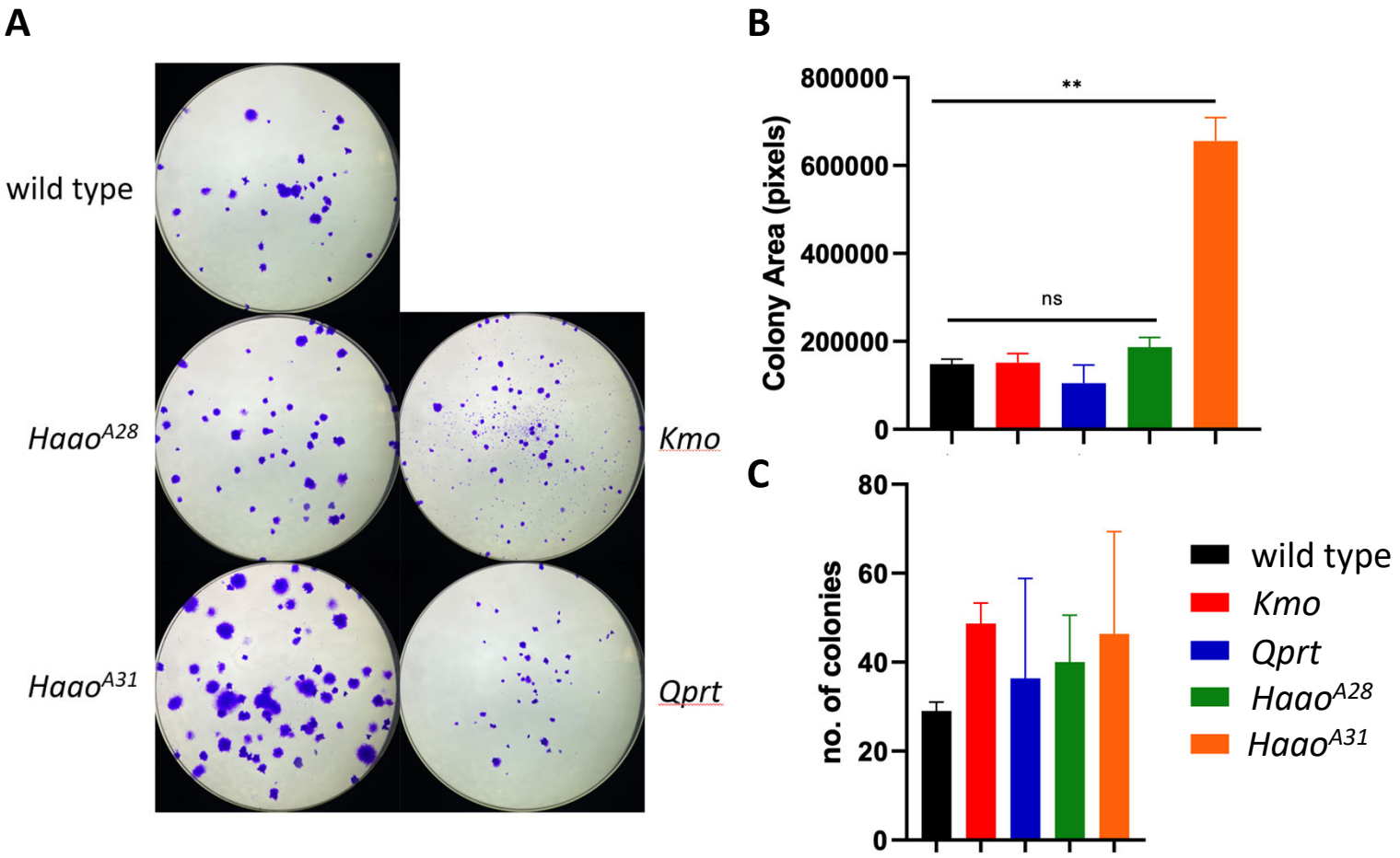

Figure 7. Renca^{Luc} cell colony formation is differentially affected by knockout of *Haao*, *Kmo*, or *Qprt*. Knockout of *Haao* (cell line A31), but not *Kmo* or *Qprt*, can significantly increases colony size but not colony number in a colony formation assay. Unlike *Haao*$^{-/-}$ cell line A31, cell line A28 did not show increase colony size, suggesting underlying differences in behavior that may imply underlying genetic or epigenetic differences for these independently generated cell lines. *Kmo*$^{-/-}$ cells showed a trend toward increased colony number that did not reach significance. (**A**) Representative images of colonies for each cell line. Quantification of colony (**B**) area and (**C**) number from each well across images. * $p < 0.05$, ** $p < 0.01$, *** $p < 0.001$, two-tailed Welch's t test with Holm multiple test correction.

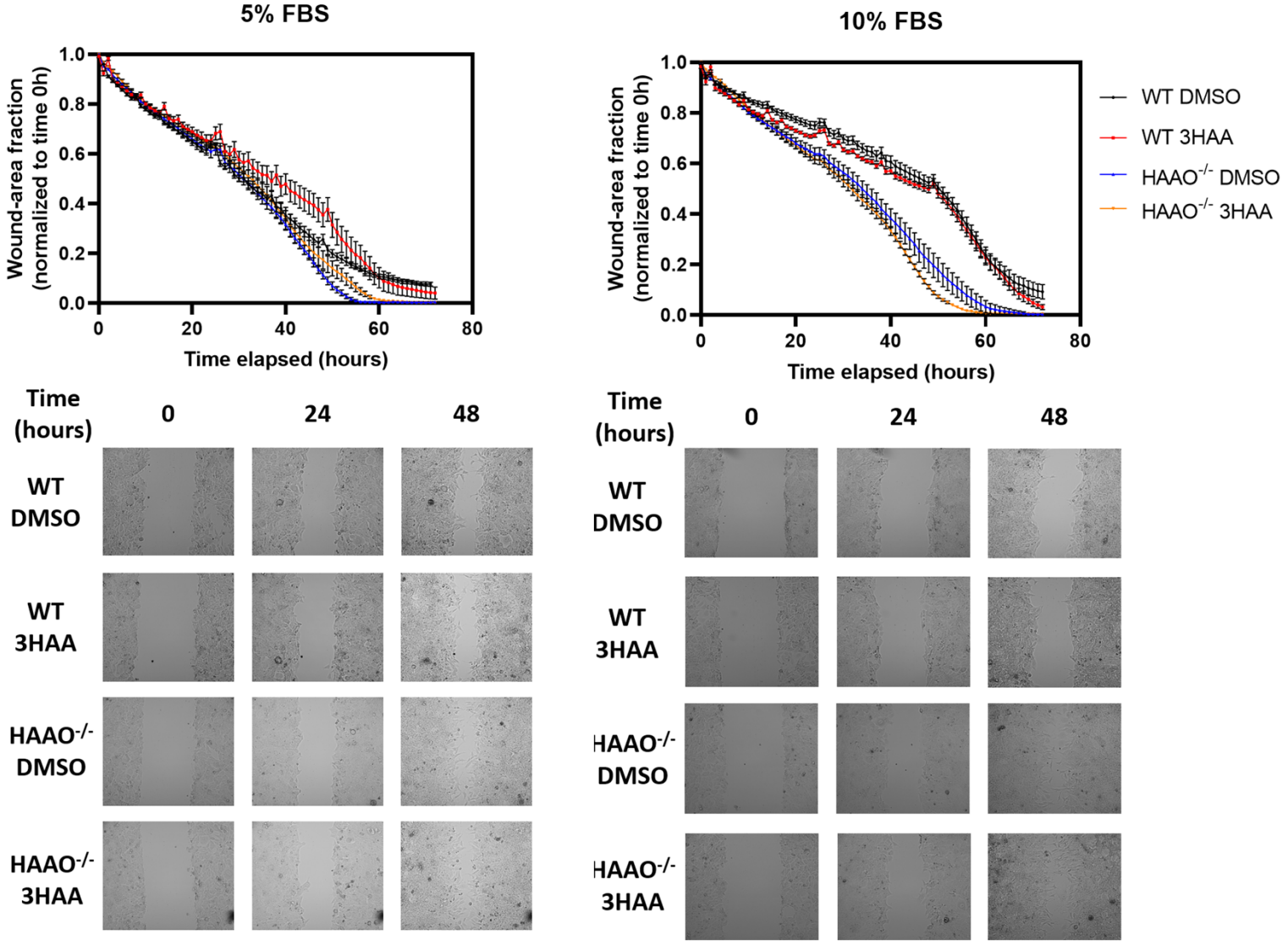

Figure 8. *Haao* knockout promotes migration and/or proliferation of Renca^{Luc} cells in a nutrient-dependent manner. *Haao*$^{-/-}$ Renca^{Luc} cells more rapidly colonize available culture area than wild type cells in a scratch/wound healing assay when cultured with 5% FBS. The difference is more distinct in 10% FBS. Media supplementation of 3HAA moderately slows growth in 5% FBS. Lower panels show representative images of scratch assays at 0, 24, and 48 hours. Upper panels show automated quantification of would area for images taken at 20 minute intervals for 72 hours following initiation of the scratch. All values are normalized to the initial scratch area.

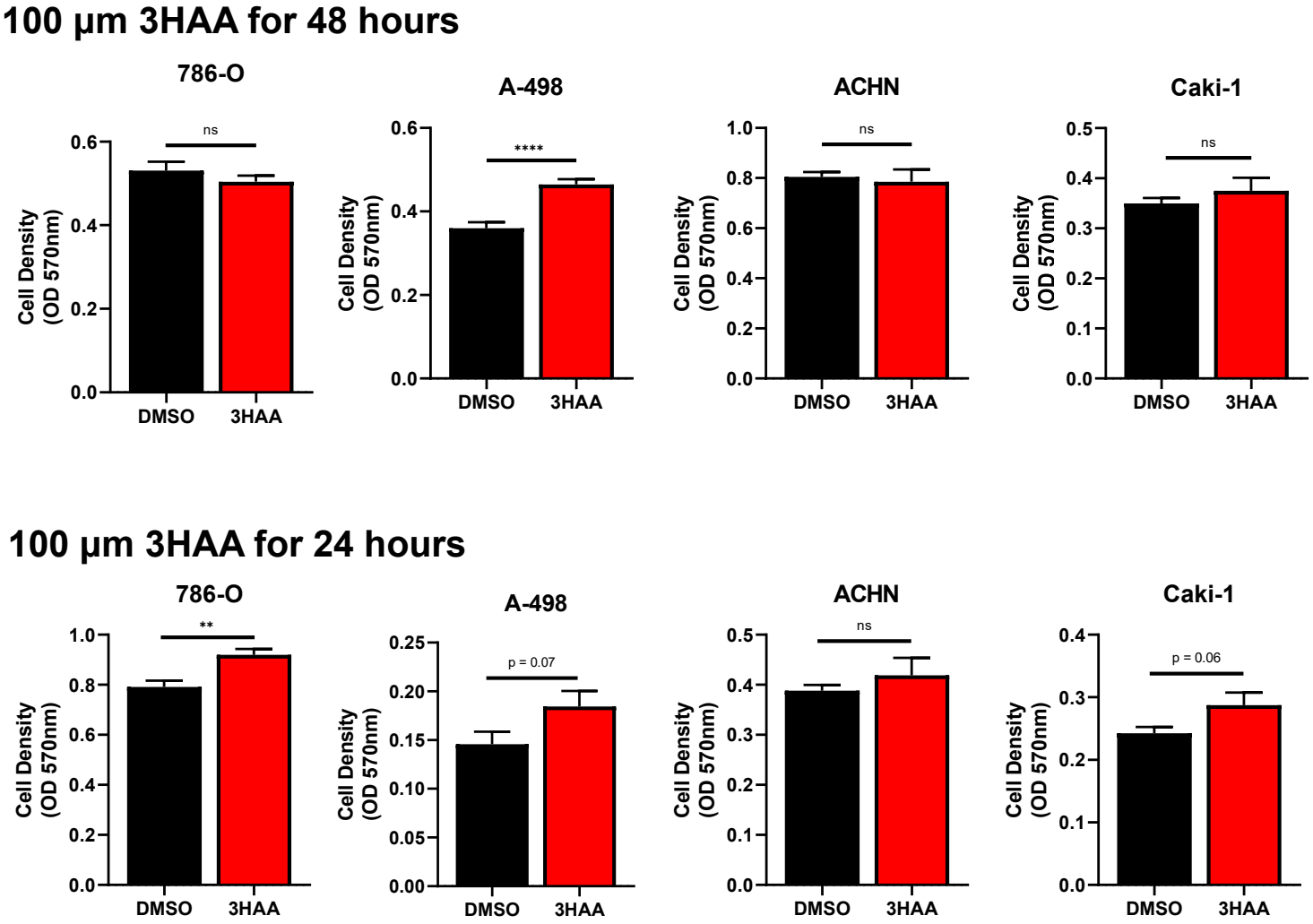

Figure 9. 3HAA supplementation increases growth rate in some human RCC cell lines. Optical density measured after 24 or 48 hours of 3HAA treatment for four human RCC lines shows a modest increase in cell proliferation for 786-O and A-498 cells, but not ACHN or Caki-1 cells.

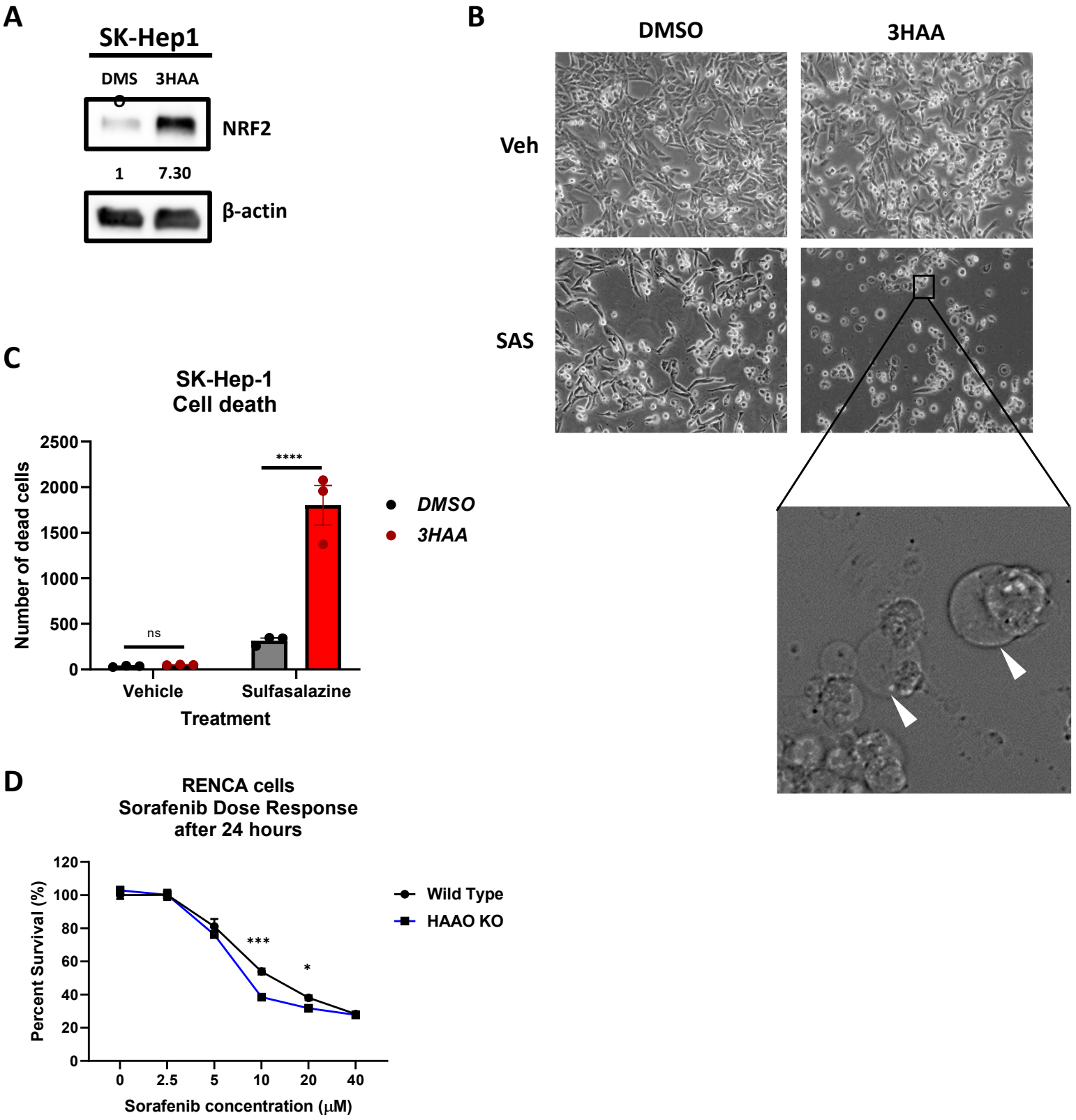

Figure 10. 3HAA sensitizes cancer cells to ferroptosis. (**A**) 3HAA induces expression of NRF2 in human SK-Hep1 cells. (**C**) 3HAA promotes cell death in human SK-Hep1 cells treated with the xCT transport inhibitor sulfasalazine (SAS) (bar graph). (**B**) 3HAA + SAS treated cells show the ballooning phenotype characteristic of ferroptosis (representative images). (**D**) Knockout of *Haao* sensitizes mouse Renca^{Luc} cells to the multi-kinase and xCT transporter sorafenib.

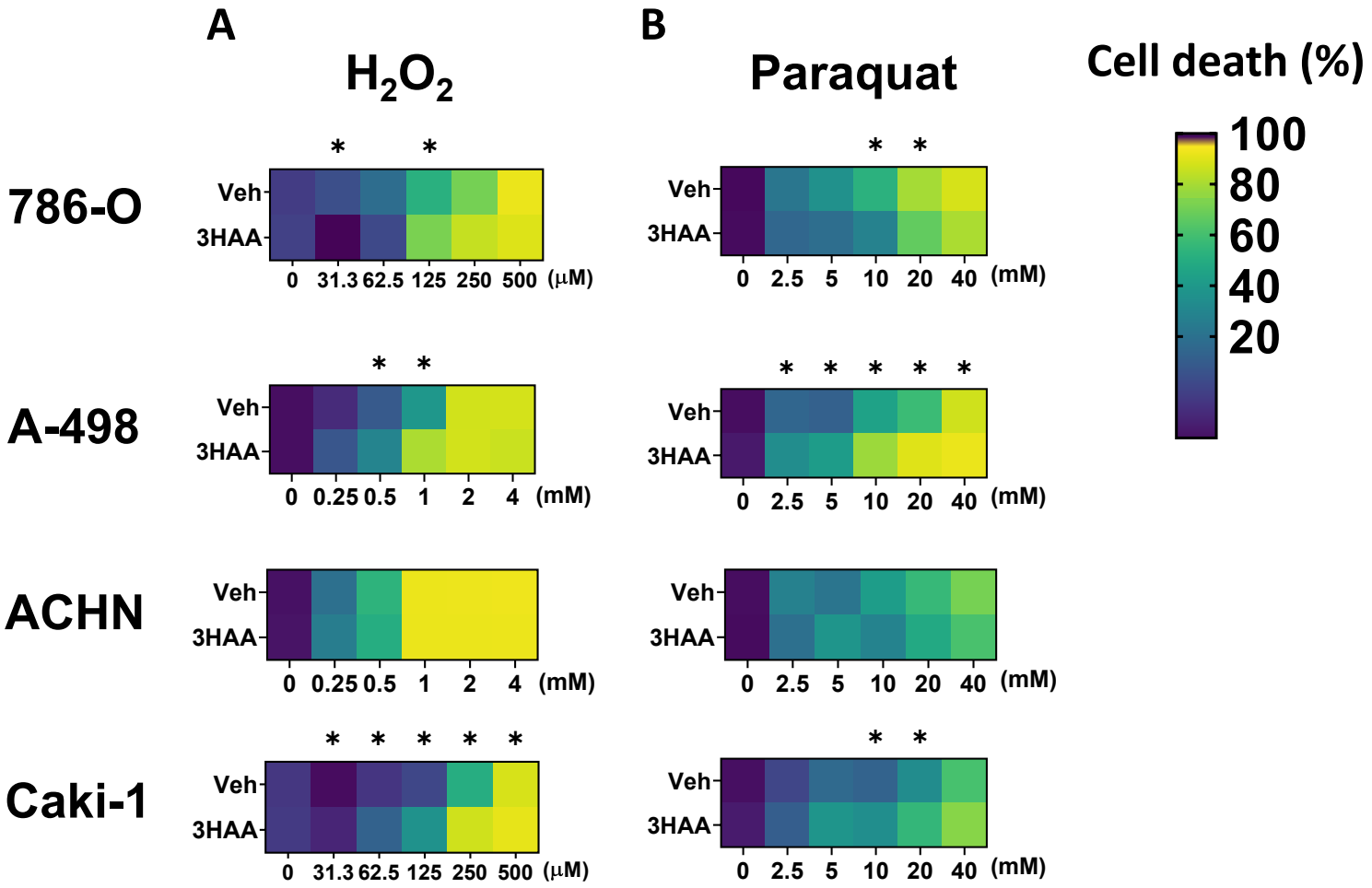

Figure 11. 3HAA does not protect consistently against RCC cell death caused by ROS-inducers hydrogen peroxide and paraquat. Heatmaps depicting the dose-dependent toxicity of (**A**) hydrogen peroxide or (**B**) paraquat, in a panel of several human RCC cell lines 786-O, A-498, ACHN, and Caki-1. * $p < 0.05$, two-tailed Welch's t-test with Holm multiple test correction method.

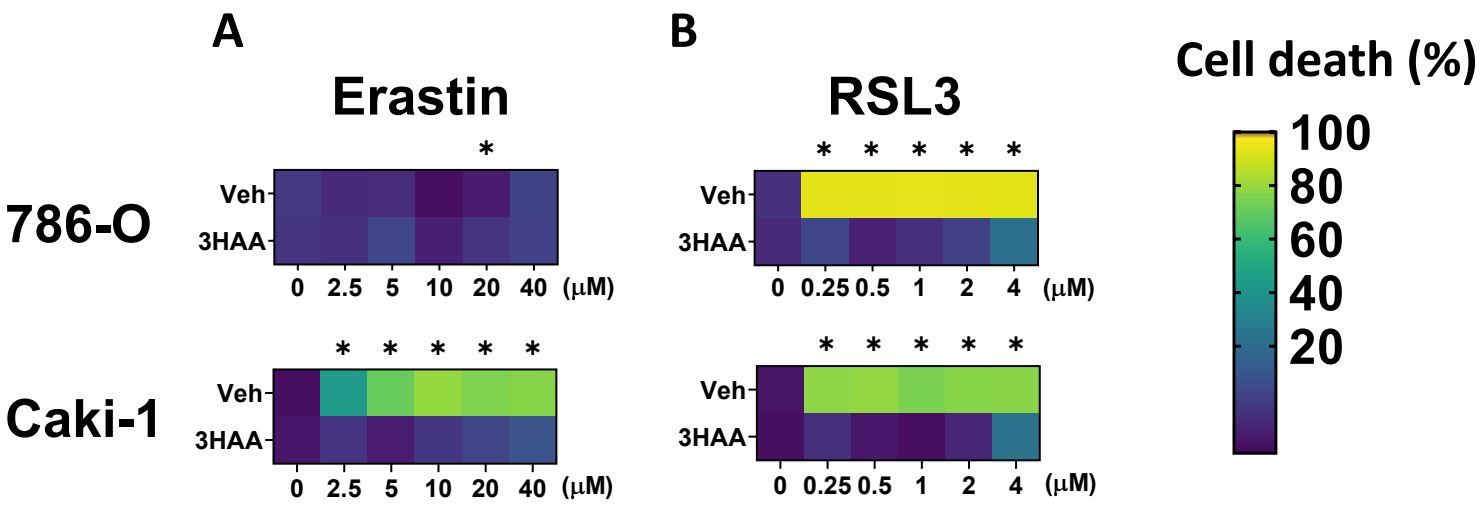

Figure 12. 3HAA significantly protects RCC cells against ferroptosis inducers Erastin and RSL3. Heatmaps depicting the dose-dependent toxicity of
(**A**) erastin or (**B**) RSL3, in human RCC cell lines 786-O and Caki-1. 786-O were insensitive to erastin with or without 3HAA. * $p < 0.05$, two-tailed Welch's t-test with Holm multiple test correction method.

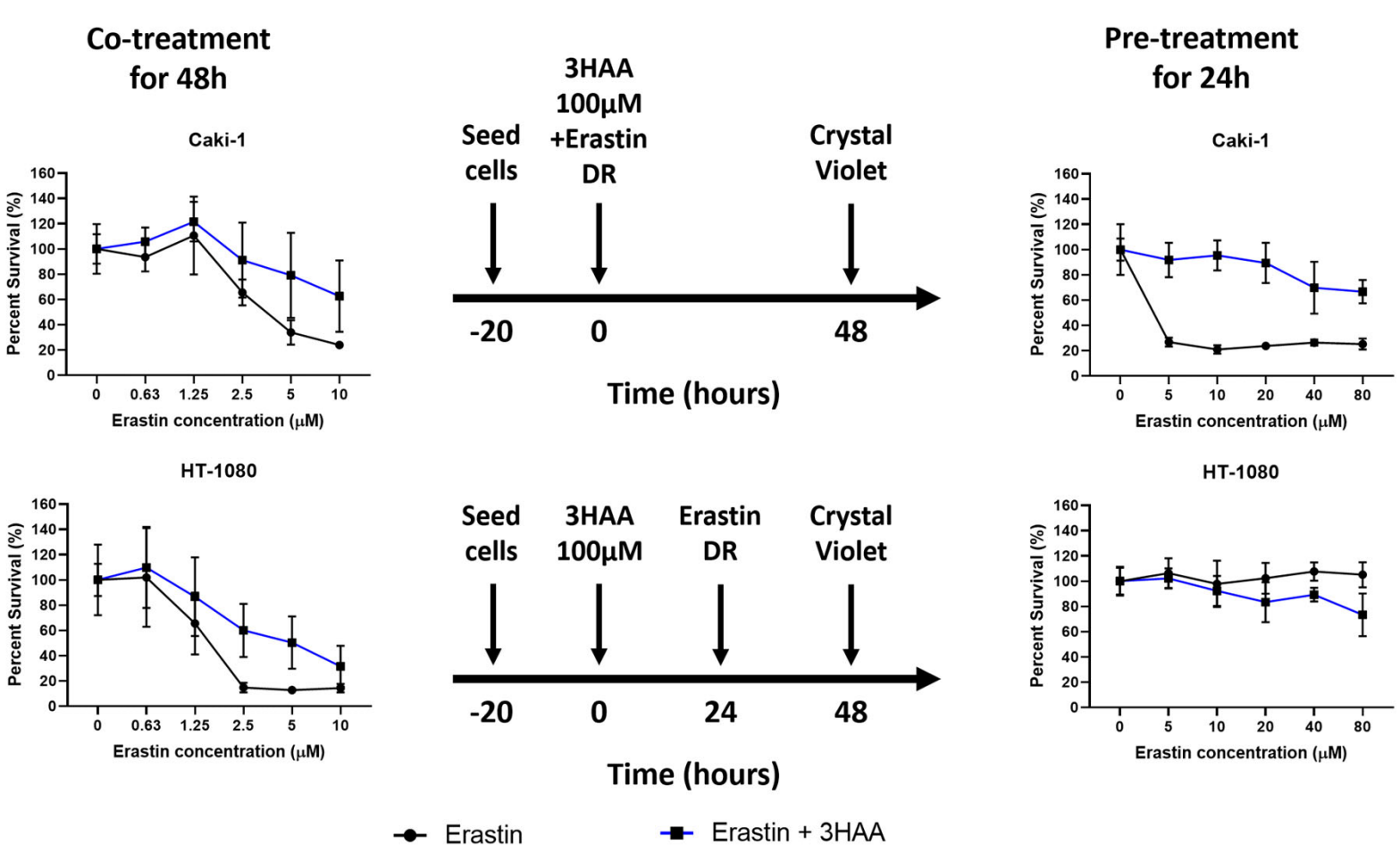

Figure 13. 3HAA relationship with ferroptosis is complex. Both the degree and direction of effect for the influence of 3HAA on ferroptosis sensitivity vary both across cell line and with treatment timing. Two examples are provided for Caki-1 and HT-1080 cells either pretreated with 3HAA prior to the specific xCT transporter inhibitor erastin or co-treatment with 3HAA and erastin.

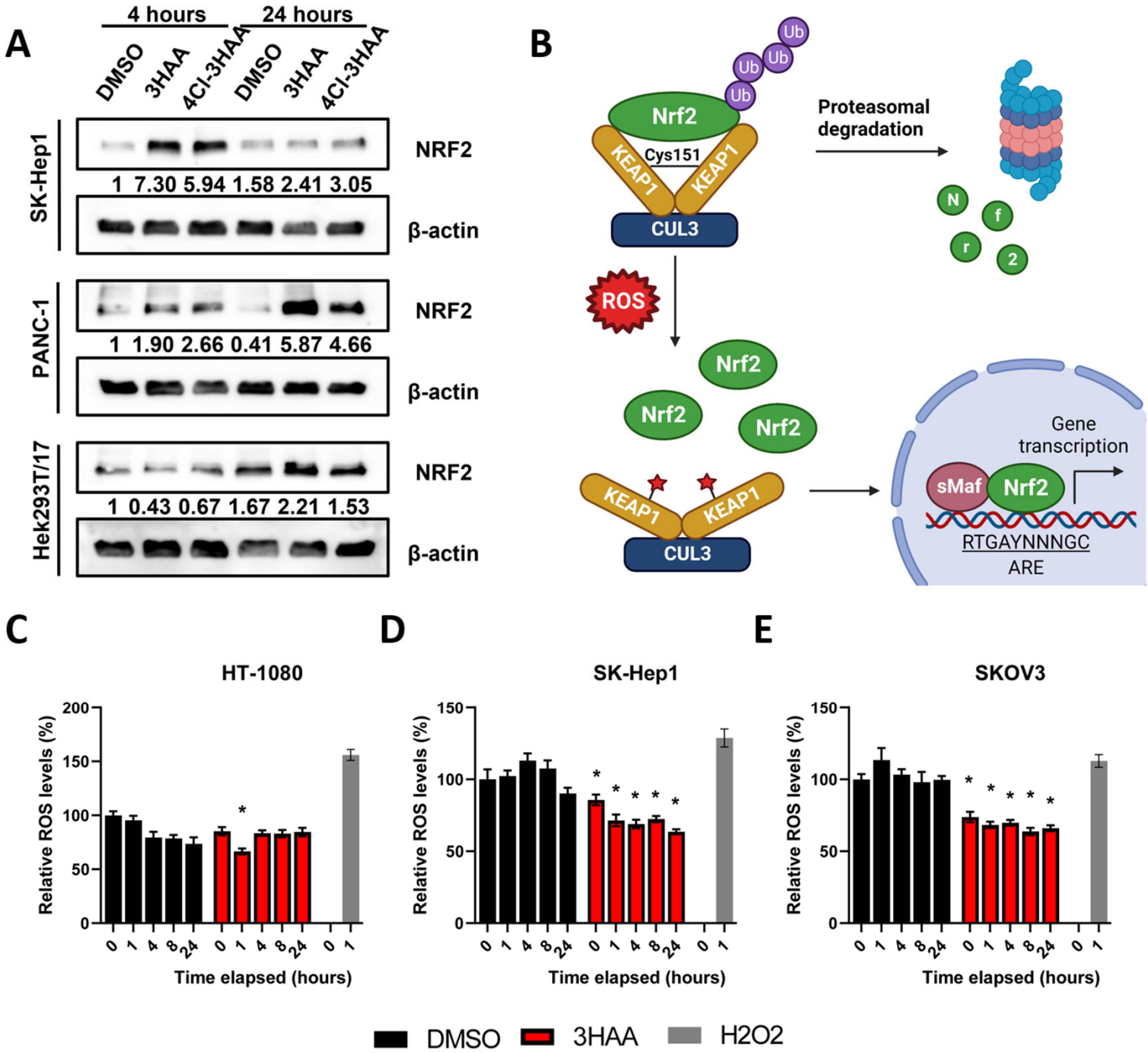

Figure 14. 3HAA induces Nrf2 accumulation but does not increase endogenous production of ROS. (**A**) Protein expression levels of Nrf2 and β-actin as a loading control were determined by Western blot. (**B**) Schematic diagram of Nrf2 upregulation by disrupt binding with KEAP1. (**C-E**) Endogenous ROS levels determined in a time dependent manner (0, 1, 4, 8 and 24 hours) by treating 3 cancer cell lines with 100 µM 3HAA. 30 minutes before collecting data, cells were treated with H_2DCFDA at a final concentration of 20 µM. Fluorescence values were determined by microplate reader measurement of 8 individual wells in a 96-well plate format. * $p < 0.05$, two-tailed Welch's t-test with Holm multiple test correction method.

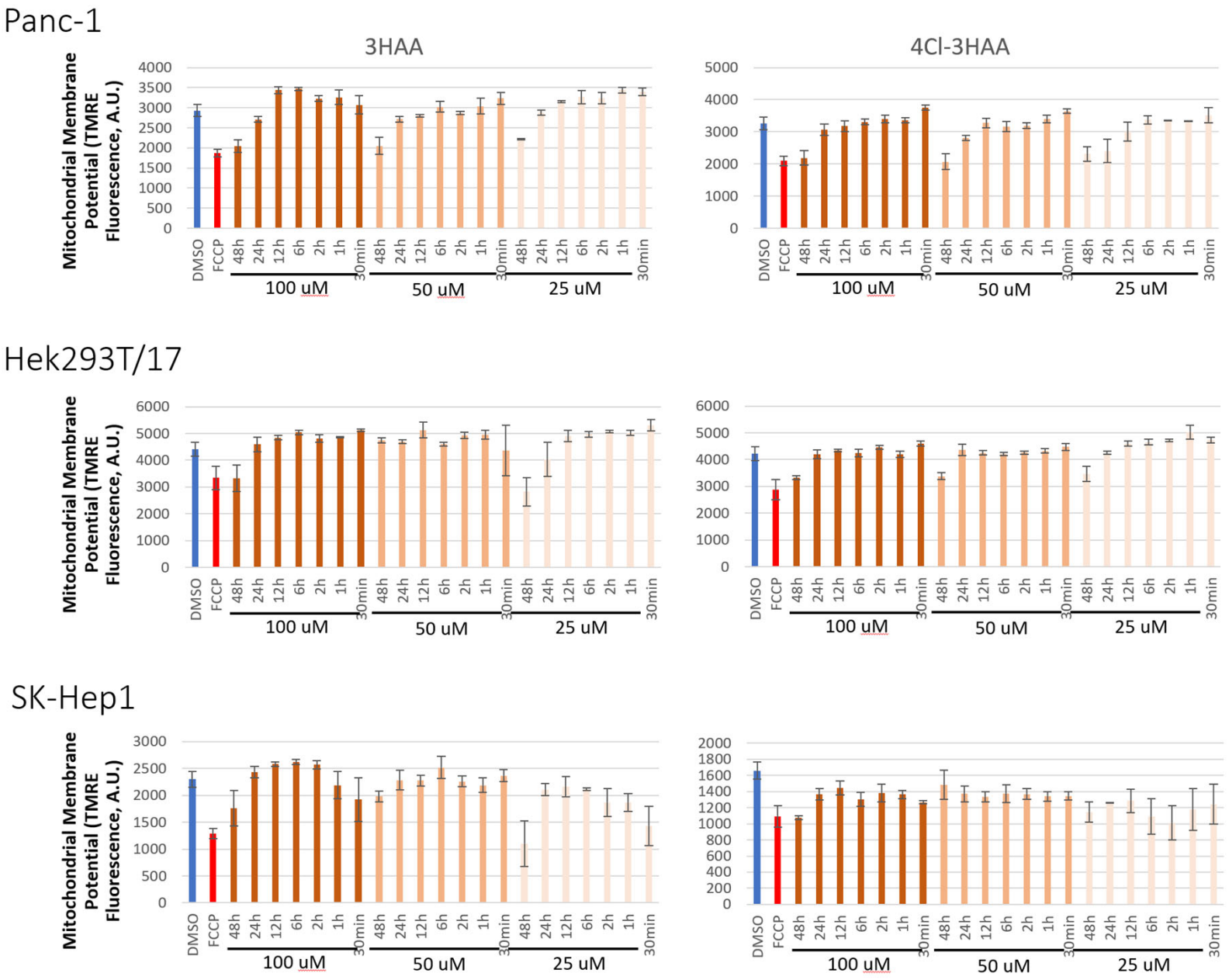

Figure 15. 3HAA or HAAO inhibition elevates mitochondrial membrane potential. Human Panc-1, Hek293T/17, or SK-Hep1 cells show a decrease in mitochondrial membrane potential on par with FCCP treatment after 48 hours following supplementation with either the endogenous metabolite 3HAA or the HAAO inhibitor 4Cl-3HAA.

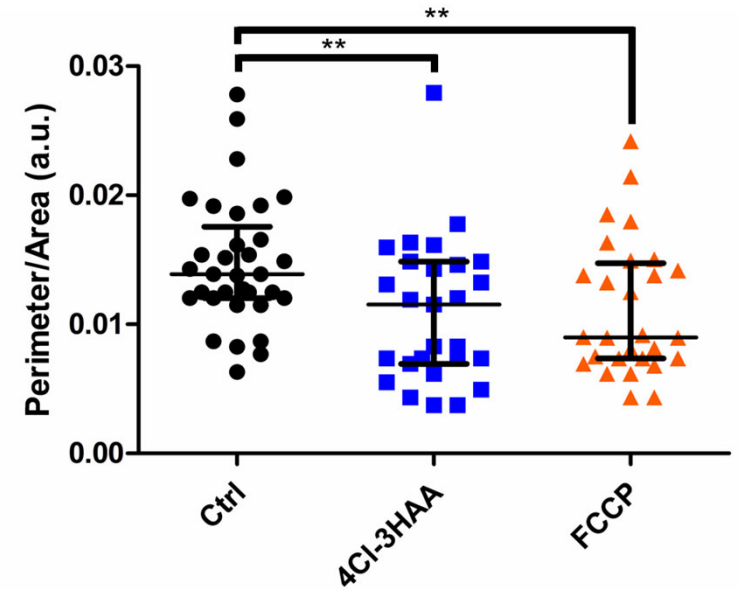

Figure 16. HAAO inhibition with 4Cl-3HAA promotes mitochondrial fission. Quantification of mitochondrial perimeter/area ratio following TMRE staining in human Caki-1 RCC cells.

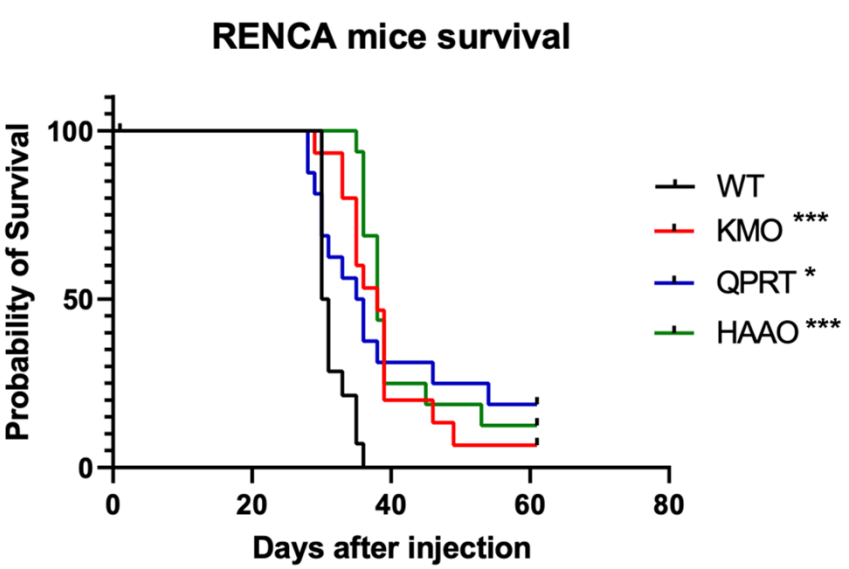

Figure 17. Inhibiting kynurenine metabolism in Renca tumor cells promotes animal survival. Kaplan-Meier survival curves for BALB/cByJ mice receiving orthotropic injections of wild type, *Haao*$^{-/-}$, *Kmo*$^{-/-}$, or *Qprt*$^{-/-}$ Renca^{Luc} cells in the left kidney. * $p < 0.05$, * $p < 0.01$, * $p < 0.001$ log rank test vs. wild type.

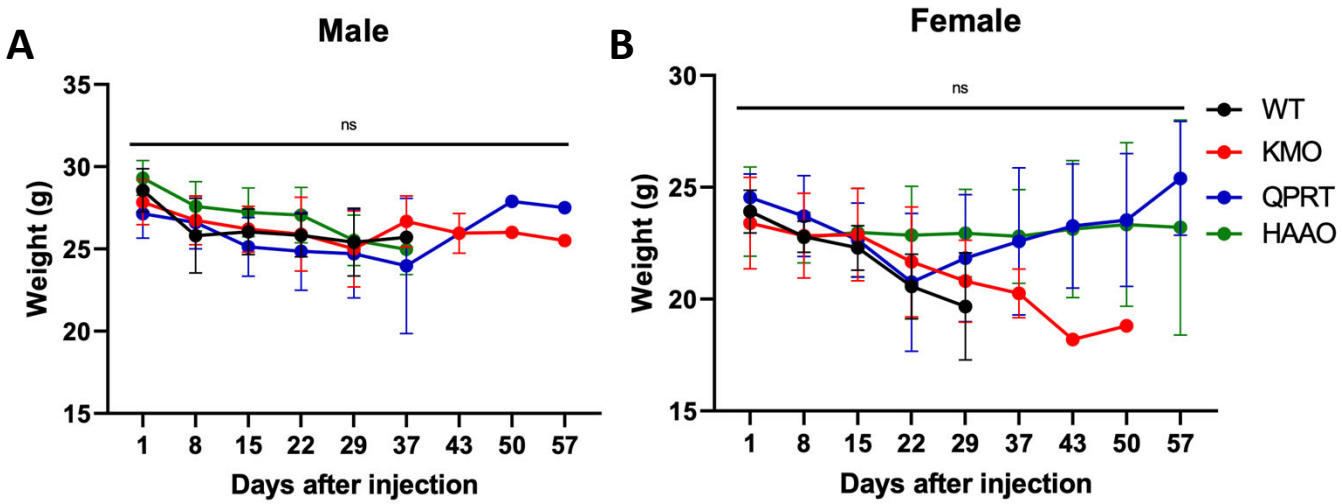

Figure 18. Inhibiting kynurenine metabolism in Renca tumor cells does not affect body weight. Body weight measured weekly in (**A**) male and (**B**) female BALB/cByJ mice receiving orthotropic injections of wild type, *Haao*$^{-/-}$, *Kmo*$^{-/-}$, or *Qprt*$^{-/-}$ Renca^{Luc} cells in the left kidney. * $p < 0.05$, * $p < 0.01$, * $p < 0.001$ two-tailed Welch's t test vs. timepoint-matched wild type.

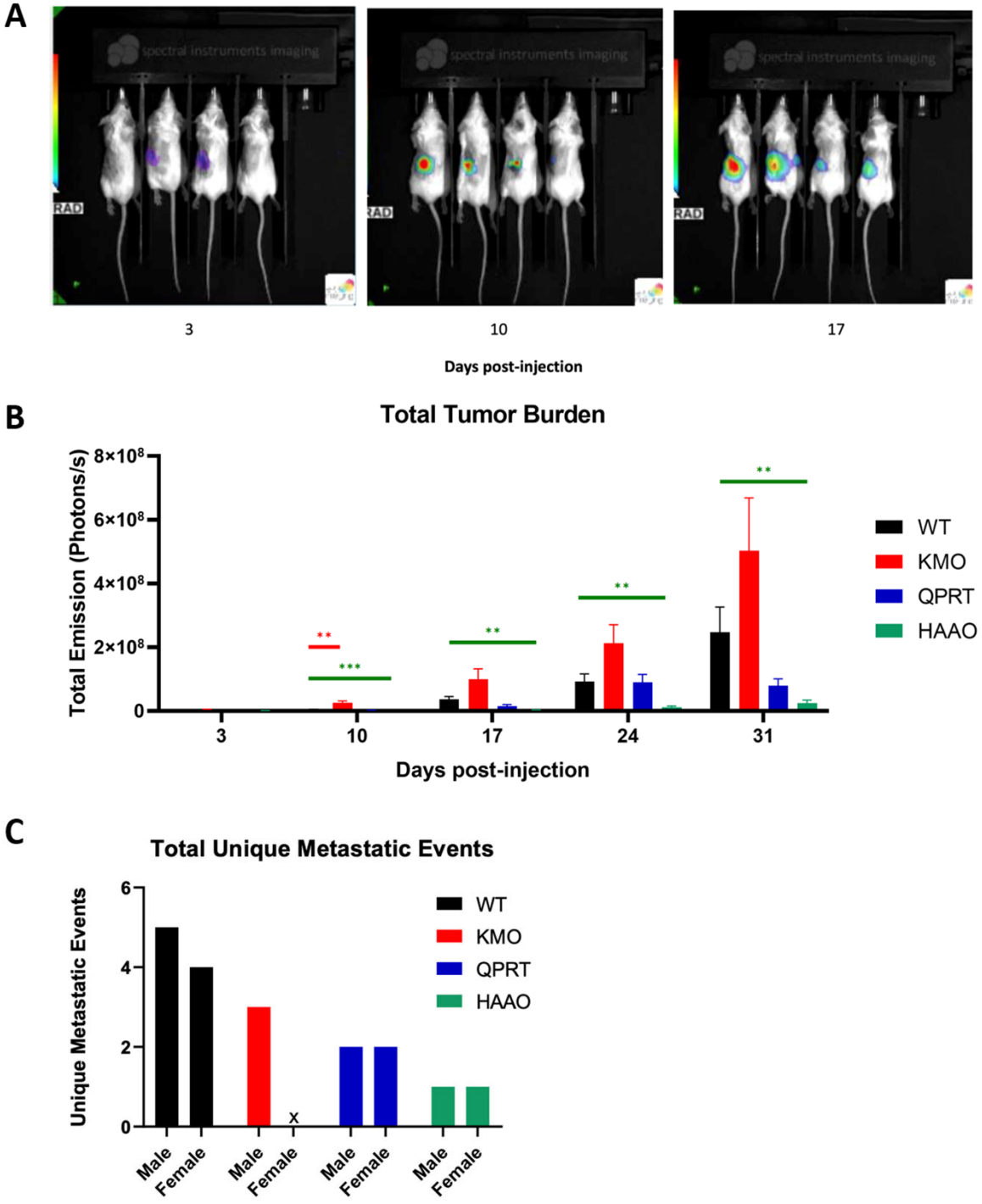

Figure 19. *Haao* knockout in Renca tumor cells limits tumor growth *in vivo*. (**A**) Representative images of bioluminescence data for BALB/cByJ mice receiving orthotropic injections of wild type, *Haao*$^{-/-}$, *Kmo*$^{-/-}$, or *Qprt*$^{-/-}$ Renca^{Luc} cells in the left kidney. (**B**) Quantification of total bioluminescence emission across images, reflecting total tumor burden. (**C**) Quantification of unique metastatic events detected in bioluminescence images across all time points. * $p < 0.05$, * $p < 0.01$, * $p < 0.001$ two-tailed Welch's t test vs. timepoint-matched wild type.

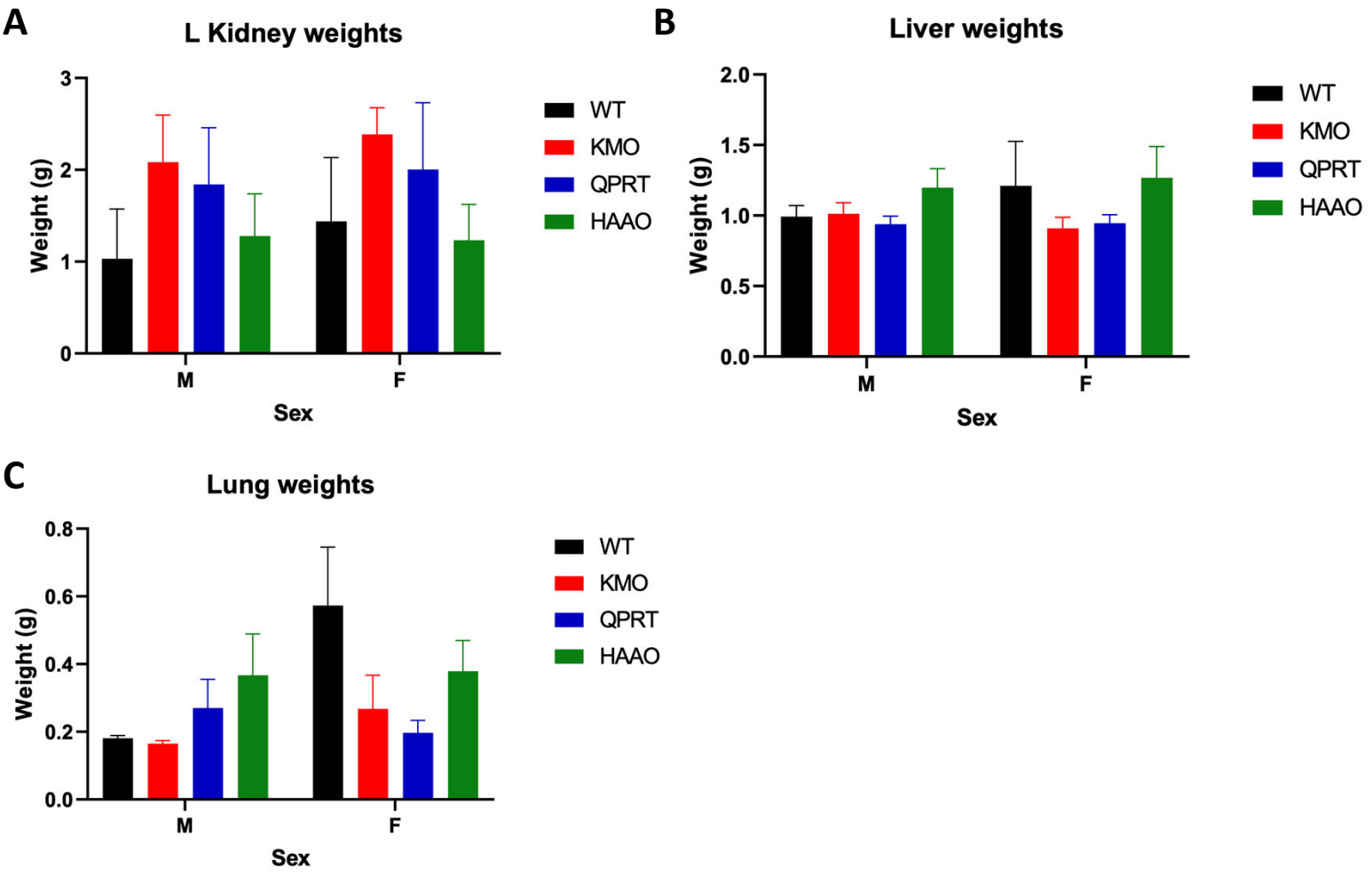

Figure 20. Inhibiting kynurenine metabolism in Renca tumor cells does not affect mean weight of kidney, liver, or lung. Wet organ weight of (**A**) left kidney (injection site), (**B**) liver, and (**C**) lung from BALB/cByJ mice 3 weeks after receiving orthotropic injections of wild type, *Haao*$^{-/-}$, *Kmo*$^{-/-}$, or *Qprt*$^{-/-}$ Renca^{Luc} cells in the left kidney. * $p < 0.05$, * $p < 0.01$, * $p < 0.001$ two-tailed Welch's t test vs. timepoint-matched wild type.

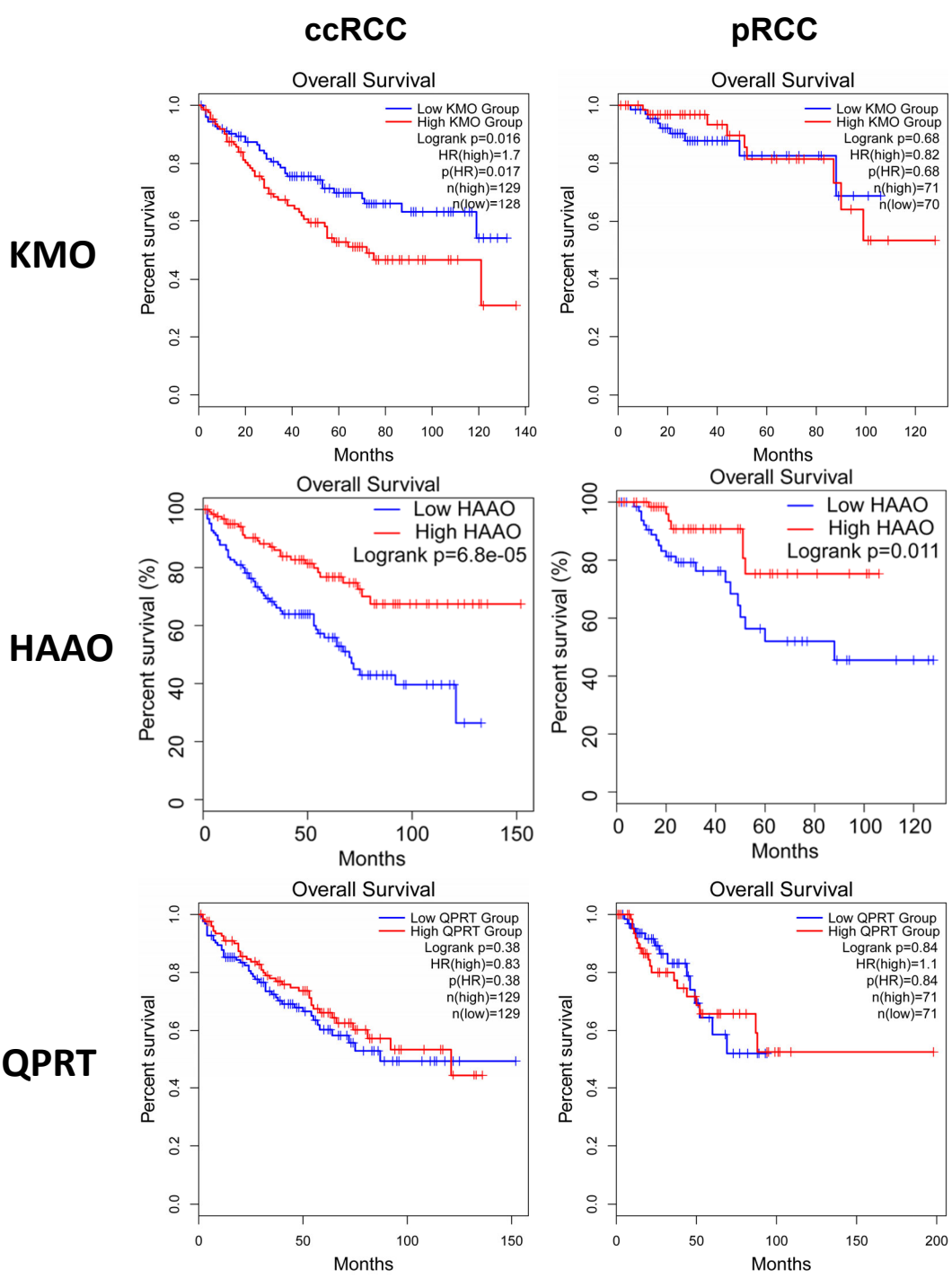

Figure 21. Expression of kynurenine pathway enzymes in RCC tumors does not clearly correlate with prognosis. Kaplan-Meier curves of overall patient survival (OS) stratified by the top and bottom quartiles of *KMO*, *HAAO*, or *QPRT* mRNA expression in clear cell RCC (ccRCC) and papillary RCC (pRCC) tumors. P values were determined by log-rank test. Data examined was from the Gene Expression Profiling Interactive Analysis (GEPIA) online database (http://gepia.cancer-pku.cn/index.html), a comprehensive platform for analysis of data from TCGA and The Genotype–Tissue Expression (GTEx) databases.

4. IMPACT:

What was the impact on the development of the principal discipline(s) of the project?

We have made several novel discoveries about the role of kynurenine metabolism in RCC pathology, particularly in the context of ferroptosis induction. There is a growing interest in the role of kynurenine metabolism in various cancers, most prominently kidney and liver cancers. Our results indicate that a straightforward model for the interaction between 3HAA and ferroptosis (e.g., actvation of NRF2 via generation of oxygen radicals) is likely to simplistic and a complete understanding will require a more comprehensive examination of the cellular redox state, labile iron pool, and baseline NRF2 activity, among other variables. We also find that the timing and dose of 3HAA relative to ferroptosis inducing drugs may be important. Finally, our *in vitro* and *in vivo* data show opposite trends in terms of cellular growth and tumor aggressiveness. This implies that cell culture does not capture important elements of the tumor microenvironment, such as the presence of immune cells, the relative importance of NAD^+ levels in culture vs. *in vivo*, or the influence of nearby normal tissue on the availability of kynurenine pathway precursor metabolites. Future studies should seek to evaluate these variables and employ models that capture the most important (co-culture, 3D organoids, further *in vivo* work).

What was the impact on other disciplines?

This project is closely tied to several other projects in my laboratory related to the role of kynurenine metabolism in aging and age-associated disease. There is continuous intellectual exchange between these projects that benefits each project. The initial identification of the interaction between 3HAA and the NRF2/SKN-1 pathway was made in the context of stress resistance in *C. elegans*, which led to the work on these processes in the context of ferroptosis in RCC cells. In turn, the preliminary work looking at the impact of 3HAA on ferroptosis sensitivity and the interaction with NRF2 and oxidative stress has led to a similar set of experiments in the context of *C. elegans* aging. We are similarly looking at the interaction between 3HAA and iron homeostasis in the context of bacterial innate immunity in *C. elegans* and mammalian cell culture. Based on the work in this project, we are looking at the activation of NRF2/SKN-1 in the immune response. Beyond my laboratory, kynurenine metabolism is of increasing interest across a range of other cancer types (liver and pancreas in particular) and diseases (neurodegenerative, cardiovascular disease). The molecular interactions identified in this work are relevant to the impact of 3HAA and other kynurenine pathway enzymes and metabolites across these disciplines.

What was the impact on technology transfer?

Nothing to Report.

What was the impact on society beyond science and technology?

Nothing to Report.

5. CHANGES/PROBLEMS:

Changes in approach and reasons for change

We have multiple projects looking at different aspects of kynurenine metabolism in aging and age-associated disease. As a consequence, our molecular models for how the system interacts with other biology are evolving rapidly. Around the time this award was funded, we had converging evidence from several other projects looking at elements of aging and age-associated immune decline that the kynurenine pathway enzyme 3-hydroxyanthanilic acid dioxygenase (HAAO) and its substrate, 3-hydroxyanthranilic acid (3HAA), interact with both iron homeostasis and the Nrf2 oxidative stress response pathway. This is important context for understanding RCC pathology and therapy, because sorafenib is used as a first- or second-line therapy for patients with metastatic RCC. While sorafenib is used primarily as a multi-kinase inhibitor, it can also promote ferroptosis by inhibiting the xCT antiporter, thus preventing glutathione production by limiting import of its precursor, cystine.

Based on this evidence, we made two minor changes to our overall approach. First, we are now including HAAO knockout and 3HAA supplementation as two additional molecular targets in our cell culture work. HAAO was already on our short list when writing the original proposal for this award, and these additions are in line with the headline goals of the project. In fact, HAAO has a specific advantage, in that HAAO knockdown specifically elevates concentrations of its substrate 3HAA. By comparing HAAO knockout to 3HAA supplementation, we have means to compare downstream consequences of inhibiting or upregulating NAD^+ production, respectively. KYNU is less well suited for this role because it carries out two distinct reactions in the pathway and knockdown results in the buildup of two metabolic products, 3-hydroxykynurenine and kynurenine. In a similar vein, emerging evidence implicated KMO in other forms of kidney pathology. As a consequence, we included both *Haao* and *Kmo* in our CRISPR knockout target list in addition to the genes originally proposed in this work (supported by an internal pilot award). The CRISPR knockout strategy was successful for *Haao*, *Kmo*, and *Qprt*. Because additional rounds of CRISPR would add cost, and these genes fulfilled our original conceptual goals, we continued with these three.

Second, we were examining how each kynurenine pathway intervention alters the response of cells to erastin, a more specific xCT antiporter that does not have the potentially confounding multi-kinase inhibition properties of sorafenib, and RSL3, a specific inhibitor of the cells ability to utilize GSH as an antioxidant. We made a minor expansion to examine key phenotypes using these molecules in the context of ferroptosis. However, this also added an important contextual element to our study that will provide mechanistic insight, namely the impact of altered *de novo* NAD^+ synthesis on the response of RCC cells to therapeutic challenge.

These modifications only modestly increase the cost of cell culture in terms of reagents and supplies. These costs were offset by our recent acquisition of a spinning disk confocal microscope (through a different funding source) that allowed us to conduct most microscopy-based assays in our laboratory without having to incur core services fees. We did not have the resources to expand

the mouse studies to include these new treatment categories. Instead, based on the cell culture data we select the three most promising Renca^{Luc} knockout cell lines and proceed to the mouse studies with just this subset.

Actual or anticipated problems or delays and actions or plans to resolve them

The construction of the Renca^{Luc} CRISPR knockout cell lines took substantially longer than anticipated, which in turn delayed most of the cell culture and mouse work outlined in the Statement of Work. Based on this delay, we requested and were granted a one year no-cost extension to complete the work. While waiting for the cell lines, we tested all methods in the work that we did not have previous experience with, optimized our sample collection for mass spectrometry, and characterized several aspects cell growth and behavior in HAAO knockout or 3HAA supplemented cells. With the extension, we were able to generate the needed cell lines proceed original plan of action on a delayed timeline, with the modifications noted above.

Changes that had a significant impact on expenditures

Nothing to Report.

Significant changes in use or care of human subjects, vertebrate animals, biohazards, and/or select agents

Nothing to Report.

Significant changes in use or care of human subjects

Nothing to Report.

Significant changes in use or care of vertebrate animals

Nothing to Report.

Significant changes in use of biohazards and/or select agents

Nothing to Report.

6. PRODUCTS:

- **Publications, conference papers, and presentations**

Journal publications.

Castro-Portuguez R, Raymond KM, Thullen E, Hendrickson AM, Freitas S, Hull B, Meyers JB, Thorns N, Gardea EA, Dang H, Espejo LS, Sutphin GL. Inhibition of haao-1 enhances oxidative stress response by activating hormetic redox signaling in C. elegans. bioRxiv 2023.02.16.528568. doi: 10.1101/2023.02.16.528568 (preparing submission for Redox Biology).

Castro-Portuguez R, Miller KM, Thorns N, Sutphin GL. 3HAA prevents ferroptosis but fails to prevent hydrogen peroxide- and paraquat-induced cell death (preparing for submission).

Castro-Portuguez R, Miller KM, Rounseville S, Thorns, N, Dang H, Sutphin GL. Tumor kynurenine pathway mutation differentially affect in vitro and in vivo behavior of renal cell carcinoma (preparing for submission).

Books or other non-periodical, one-time publications

Oral Presentations

Castro-Portuguez R. The Emerging Role of Kynurenine Pathway in Regulating Nrf2 and Ferroptosis. *Cancer Biology Student Research Colloquium, University of Arizona.* Tucson, AZ. 25 August 2022.

Castro-Portuguez R. The Kynurenine Derivative 3HAA Sensitizes Hepatocellular Carcinoma to Ferroptosis. *Research Day, Future of Medical Innovations I, University of Arizona*. Tucson, AZ. 4 May 2022.

Castro-Portuguez R. A Tale of Two Amino Acids: From Tryptophan Metabolism to Cysteine Addiction. *Tim and Diane Bowden Research Symposium, Cancer Biology Retreat*. Tucson, AZ. 18 March 2022.

Sutphin GL. Targeting kynurenine metabolism in cancer. *University of Arizona Cancer Center (UACC) Retreat, University of Arizona.* Tucson, AZ. 20 November, 2021.

Castro-Portuguez R. The Kynurenine Derivative 3HAA Sensitizes Hepatocellular Carcinoma to Ferroptosis. *Cancer Biology Student Research Colloquium, University of Arizona*. Tucson, AZ. 23 September 2021.

Other publications, conference papers and presentations. *Identify any other publications, conference papers and/or presentations not reported above. Specify the status of the publication as noted above. List presentations made during the last year (international, national, local societies, military meetings, etc.). Use an asterisk (*) if presentation produced a manuscript.*

Oral Presentations

Castro-Portuguez R. The Emerging Role of Kynurenine Pathway in Regulating Nrf2 and Ferroptosis. *Cancer Biology Student Research Colloquium, University of Arizona.* Tucson, AZ. 25 August 2022.

Castro-Portuguez R. The Kynurenine Derivative 3HAA Sensitizes Hepatocellular Carcinoma to Ferroptosis. *Research Day, Future of Medical Innovations I, University of Arizona*. Tucson, AZ. 4 May 2022.

Castro-Portuguez R. A Tale of Two Amino Acids: From Tryptophan Metabolism to Cysteine Addiction. *Tim and Diane Bowden Research Symposium, Cancer Biology Retreat*. Tucson, AZ. 18 March 2022.

Sutphin GL. Targeting kynurenine metabolism in cancer. *University of Arizona Cancer Center (UACC) Retreat, University of Arizona.* Tucson, AZ. 20 November, 2021.

Castro-Portuguez R. The Kynurenine Derivative 3HAA Sensitizes Hepatocellular Carcinoma to Ferroptosis. *Cancer Biology Student Research Colloquium, University of Arizona*. Tucson, AZ. 23 September 2021.

Sutphin GL. Extending healthy lifespan with 3HAA. *2023 Gerontological Society of America Annual Meeting.* Indianapolis, IN. 5 November, 2023.

- **Website(s) or other Internet site(s)**

  Nothing to report.

- **Technologies or techniques**

  Nothing to report.

- **Inventions, patent applications, and/or licenses**

  Nothing to report.

- **Other Products**

  Nothing to report.

7. PARTICIPANTS & OTHER COLLABORATING ORGANIZATIONS

What individuals have worked on the project?

Name:	George Sutphin
Project Role:	PI
Researcher Identifier (ORCID):	0000-0002-3659-4678
Nearest person month worked:	1
Contribution to Project:	Dr. Sutphin oversees the administrative aspect of this project, arranging meetings, interacting with core services, guiding conceptual development, and communicating findings.
Funding Support:	This award

Name:	Jose Raul Castro-Portuguez
Project Role:	Graduate Student
Researcher Identifier (ORCID ID):	0000-0001-7037-8859
Nearest person month worked:	6
Contribution to Project:	Mr. Castro-Portuguez is the primary researcher working on this project. He plans and conducts experiments, works with Dr. Sutphin to monitor and develop the conceptual goals of the project, and conducts primary processing, analysis, and presentation of collected data.
Funding Support:	This award

Has there been a change in the active other support of the PD/PI(s) or senior/key personnel since the last reporting period?

Nothing to report.

What other organizations were involved as partners?

Nothing to report.

8. SPECIAL REPORTING REQUIREMENTS

COLLABORATIVE AWARDS:

N/A

QUAD CHARTS:

N/A

9. APPENDICES:

Nothing to report.